

University of Alabama in Huntsville

LOUIS

Theses

UAH Electronic Theses and Dissertations

2023

The spiral generator : theory and methods for modeling and fabrication

Jacob Kinsey

Follow this and additional works at: <https://louis.uah.edu/uah-theses>

Recommended Citation

Kinsey, Jacob, "The spiral generator : theory and methods for modeling and fabrication" (2023). *Theses*. 525.

<https://louis.uah.edu/uah-theses/525>

This Thesis is brought to you for free and open access by the UAH Electronic Theses and Dissertations at LOUIS. It has been accepted for inclusion in Theses by an authorized administrator of LOUIS.

**THE SPIRAL GENERATOR: THEORY AND METHODS FOR
MODELING AND FABRICATION**

Jacob Kinsey

A THESIS

**Submitted in partial fulfillment of the requirements
for the degree of Master of Science in Aerospace Systems Engineering
in
The Department of Mechanical and Aerospace Engineering
to
The Graduate School
of
The University of Alabama in Huntsville
August 2023**

Approved by:

Dr. Jason Cassibry, Research Advisor

Dr. Gabe Xu, Committee Member

Dr. Sivaguru Ravindran, Committee Member

Dr. Keith Hollingsworth, Department Chair

Dr. Shankar Mahalingam, Dean

Dr. Jon Hakkila, Graduate Dean

Abstract

THE SPIRAL GENERATOR: THEORY METHODS FOR MODELING AND FABRICATION

Jacob Kinsey

**A thesis submitted in partial fulfillment of the requirements
for the degree of Master of Science in Aerospace Systems Engineering
Mechanical and Aerospace Engineering
The University of Alabama in Huntsville
August 2023**

This thesis attempts to confront shortcomings of spiral generator knowledge of testing at low voltages, design techniques of spiral generators, and fabrication methods. To achieve this, basic fabrication methods were employed for generators to be tested at low and high voltage. This effort allowed development of a simple two-frequency model and winding machine. This two-frequency model depicts output waveform amplitude as a scaler of charging voltage and has been found to be adequate for using the model in comparison to less trivial models which can be less accurate in time-domain behavior. An updated winding machine was proposed as a result of the exploration of fabrication methods. This also shows that design of a decently efficient spiral generator requires broad knowledge of the theory of operation and interactions with geometric parameters and electrical characteristics. For the spiral generator to be widely adopted for commercial use, more methods modelling multiplication efficiency factors will need to be developed.

Acknowledgements

Thank you to Zac Shotts for wonderful guidance with the wealth of experience he provided to allow this research to progress. Without his help on the function and theory of operation on the spiral generator, this effort would have been drawn out.

Thank you to Jason Cassibry for the mentoring and academic guidance throughout graduate school and for the opportunity to work on this research in the UAH CAPP Lab. It has been a highlight of my higher education.

Table of Contents

Abstract.....	ii
Acknowledgements	iv
Table of Contents	v
List of Figures.....	vii
Chapter 1. Introduction	1
1.1 Statement of the Problem	1
1.2 Brief Problem History	1
1.3 Objectives.....	3
1.4 Approach Summary.....	4
1.5 Thesis Synopsis.....	5
Chapter 2. Literature Survey.....	7
2.1 Works Pertaining to Spiral Generators.....	7
2.1.1 The 1964 Presentation of the Spiral Generator by R. Fitch and V. Howell.....	7
2.1.2 The 1976 Work of A. Ramrus, and F. Rose on Spiral Generators	8
2.1.3 The 1980 Work of F. Rühl and G. Herziger on Modeling Spiral Generator Behavior	9
2.1.4 The 2005 Continuation of the Work of Ramrus and Rose by F. Rose, Z. Shotts, and Z. Robert.....	10
2.1.5 The 2007 Efforts of E. Pal’chikov, E. Bichenkov and Associates Towards the Refinement of the Theoretical Model of the Spiral Generator.....	11
2.1.6 The 2007 Continuation of the Work of Schotts and Rose with the Contributions of J. Hanlon.....	13
2.1.7 The 2021 Exploration of Switch Characteristics and Modeling of Loading Effects by J. Yan, S. Parker, and Associates	14
2.1.8 The 2022 Exploration of Liquid Dielectric Use in Spiral Generators by Isaac Cohen and Associates	18
2.2 Works Pertaining to Other Vector-Inversion-Generators	19

2.2.1	The 1971 Exploration of Marx Generators by R. Fitch at Maxwell Laboratories	20
2.2.2	The 2003 Exploration of Switching Methods for Marx Generators by K. LeChien and J. Gahl.....	21
2.2.3	The 2011 Effort on Improving the Efficiency of the Marx Generator by N. Mutnitskii and V. Tatur.....	22
2.2.4	The 2000 Exploration of the Transformer-Coupled LC Generator by T. Engel and Associates	23
2.2.5	The 2020 Exploration of an Alternately Configured Transformer-Coupled LC Generator by R. Bischoff	24
Chapter 3. Methodology		26
3.1	Investigation	26
3.1.1	The Idealized Spiral Generator	26
3.1.2	Important Parameters and Electrical Characteristics	29
3.1.3	Efficiency of the Spiral Generator	32
3.1.4	Modeling Considerations of the Spiral Generator	34
3.1.5	Modeling the Time-Dependent Behavior of the Spiral Generator.....	37
3.1.6	Design Considerations	44
3.2	Materials Used.....	50
3.3	Approach Taken	53
Chapter 4. Results.....		65
Chapter 5. Conclusion		78
5.1	Conclusions Pertaining to the Hypothesis and Objectives.....	78
5.2	Conclusions of Approach and Methodology.....	79
5.3	Common Problems Faced	81
5.4	Applications for Spiral Generators.....	84
5.5	Conclusions of Experimental Results	85
5.6	Conclusions of Analytical Results	86
5.7	Final Thoughts.....	88

List of Figures

Figure 3.1	Example Configuration of a Spiral Generator	27
Figure 3.2	Internal example of vector inversion	28
Figure 3.3	Switch rise time ratio with the first efficiency factor	33
Figure 3.4	Equivalent Circuit Diagram of a Spiral Generator.	34
Figure 3.5	Equivalent Circuit Diagram Used by Rose and Shotts.....	39
Figure 3.6	Stacked Stripline Generator Configuration	45
Figure 3.7	Twin Generator Configuration	46
Figure 3.8	The PT-55 professionally manufactured Spiral Generator.....	48
Figure 3.9	Front face of the PT-55.....	49
Figure 3.10	Tektronix TDS 754D Oscilloscope	52
Figure 3.11	Winding System Used for Fabrication	55
Figure 3.12	Alignment and Friction Gate used for Winding in Progress	56
Figure 3.13	Pulley System to Replace Gate System.....	57
Figure 3.14	A 30-turn spiral generator fabricated as a first test.	58
Figure 3.15	A close up view of the layers of the 30-turn spiral generator.....	59
Figure 3.16	A close up view of the 52-turn spiral generator.	61
Figure 3.17	A Simple Adjustable Spark Gap used in Testing of the 52-Turn Spiral Generator	62
Figure 3.18	A Collection of Spiral Generators	63
Figure 4.1	Results for 30 Turn Spiral at a) 2 V with no Switch Bounce, b) 4.1 V with Switch Bounce, c) 2 V with Switch Bounce, and d) 4.1 V with Switch Bounce.	66

Figure 4.2 Experimental Results for a 30 Turn Generator, All Cases were Performed at a Charging Voltage of 4.1 V.....	67
Figure 4.3 Results for 30 Turn Spiral Generator at a) 5 V, b) 6 V, c) 7 V, d) 8 V on a Tektronix TDS 754D Oscilloscope.	68
Figure 4.4 Final Test Case for a 30 Turn Generator Charged to 9V.....	69
Figure 4.5 Comparison of Geometric Scaling of Turns	71
Figure 4.6 Comparison of Geometric Scaling of Width	72
Figure 4.7 Comparison of Geometric Scaling of Mean Diameter	73
Figure 4.8 Comparison of Geometric Scaling of Turns from Given Values	74
Figure 4.9 Comparison of Geometric Scaling of Width from Given Values	75
Figure 4.10 Comparison of Geometric Scaling of Diameter from Given Values	76

List of Tables

Table 3.1 Electrical Characteristics of Generators Explored	47
Table 4.1 Electrical Characteristics of Generators Explored	65
Table 4.2 Summarized high-voltage results of a 50-turn generator.	70

Chapter 1. Introduction

1.1 Statement of the Problem

Spiral vector inversion generators are devices that can produce high-voltage pulses with precise rise and fall times, have a relatively small footprint, and can easily be designed and fabricated in a lab space. These pulse generators are a type of pulse forming line and are promising for meeting the needs of triggering gas switches or other high voltage triggering needs [1], [2]. Unlike other pulse generators the spiral generator is very easy to construct, can be trivially massed produced, and has very low jitter. Jitter is a random variation in expected time versus an ideal time for almost any event, but it is explored with some more detail in [3]. Issues arise from difficulty in surmising the efficiency of the generator's voltage multiplication, and prediction of the time-dependent behavior of the generator's output waveform. Other than difficulties predicting the generator behavior, the generators are perfect for lab space use with little cost in time or effort to produce precise, programmable, and very high voltage pulses.

1.2 Brief Problem History

Fitch and Howell developed the first spiral generators in 1964 [4]. The application of this generator was to produce a compressed short pulse from an initial long pulse at a much higher output voltage. After this, research efforts have been making the underlying processes of the spiral generator better understood. The spiral generator has seen an increased presence in research beginning in the early 2000s, seeing early development by A. Ramrus at Maxwell Laboratories as early as 1976, where the design was presented to the Navy because of its portability and cheap construction [5]. The team at Radiance

Technologies, led by M. Franklin Rose and Z. Shotts, sought to develop spiral generators capable of multi-megawatt power levels in the early 2000s and beyond [4], [5]. In recent years these generators have seen relevant research publication as late as 2020 and 2021 by Yan Parker and associates where they explored the effects of inductivity and switch inductance as well as other parameters on spiral generators [2], [3]. Then, the most recent publication is found in 2022 by Cohen *et al* in which the viability of liquid dielectrics as the primary source of electrical insulation of a spiral generator is explored [6].

Other generators using similar operating principles of a spiral generator have been developed as well. This type of generators are called vector inversion generators. This type of generator includes Marx banks, and LC generators. Despite sharing similar operating principles, the applications of these generators tend to be quite different. Marx banks are often used for very high energy systems and take up large volumes with high maintenance cycles due to switching. LC generators suffer from similar problems. Solid-state switches are desirable but often force the choice between having even more switches or having voltages per stage at least in the case of Marx banks. LC generators can be switched with a single switch and transformers for the remaining stages. This has some advantages, but also still requires the transformers to be rated for the stage-wise voltage and still requires maintenance. The spiral generator offers some solution to this problem by only requiring one switch and if designed correctly requires little to no maintenance of the generator itself. It does however take some intelligent design to get the same energy output as that of a Marx bank.

1.3 Objectives

Research objectives for the thesis will now be defined. As the spiral generator is not so well understood by the wider community, the first objective of illustrating the function and uses of the generator is to give context on why the following objectives are important and to direct future research efforts. For the next objective this thesis shall explain the relevant equations, physics, and theory relevant to the spiral generator. The design process of the generator, and equations, and theory are elaborated on in detail. The focus is to illuminate a path for development of a spiral generator as well as alternative approaches including their strengths and weaknesses. For the third research objective, this thesis shall show and elaborate on the relevant analytical models for the physics that allow a spiral vector inversion generator to operate. A preferred model is presented as it is simpler and will work better than many complex models for generators designed for most general use cases. These models are focused upon as an objective due to the lack of publicly available models that are effective for accurately predicting a generator's behavior. As an objective, this thesis shall explain the parameters of the spiral vector inversion generator and how they impact the generator's function. This is important as many of the geometric and electrical characteristics of the generator are intertwined in an emergent manner. The next objective is that this thesis shall elaborate on methods that were and could be used to fabricate spiral vector inversion generators. Approaches for fabrication of spiral generators are discussed beginning from an entry level to fabricating one in a lab, proceeding with a more industrial level for manufacturing generators that has been utilized by other efforts, and ending with a few special cases. These details are important to know as the spiral generator is sensitive to defects, and irregularities for several reasons later discussed. For

the final objective, this thesis shall explore methods of further enhancing the outputs of a spiral vector inversion generator. Improving the output of the generators is an important topic as the efficiency of a generator is not easily predicted prior to fabrication and testing. While this is true, this is an objective as there are some simple methods to avoid common pitfalls in design that result in a lower efficiency generator. This line of discussion is completed by mentioning possible future work on modelling the efficiency of a generator using large data sets or an expansion of the preferred model presented in this work. These objectives establish a research direction which has the intent of making the spiral generator desirable for industry usage.

1.4 Approach Summary

It was first set out to fabricate a working spiral generator as a proof of concept, a baseline for further designs, and to gain knowledge on the best methods to fabricate and design them. An equivalent circuit model was procured from J. Yan and associates to provide insight and an analytical model to compare to [7]. It became clear a winding machine was needed to help manufacture the generators, leading to the first working generator design. As research began several generators were built and tested to be compared to the equivalent circuit model. It was noted that most of the results presented were at high voltages, to remove difficulties involving field grading the tests in this work were mostly performed at low voltages.

Observations made apparent a simple model for the output waveform of a spiral generator. This waveform was used to compare to those produced by the initial low voltage results, and due to the difficulty in elegantly fabricating the generators other efforts were searched to compare to their results. This was done to build further confidence in this

surprisingly simple model. The results of J. Yan's geometric scaling analysis were used to compare this model to, due to the presence of both experimental results and results produced by the model utilized in that study. This allowed for better confidence in the model without the effort of physically fabricating new generators.

1.5 Thesis Synopsis

Provided first in Chapter 2 is a summary of the literature survey into previous efforts on both spiral generators and into other forms of vector inversion generators (VIGs). This touches on the efforts of several teams in detail and was used as a reference for the designing of the objectives of this work. Chapter 2 contains description of general methods and methods of key contributors. The methods often used in other VIGs are also described there. Each work reviewed is allotted a section and are presented in chronological order.

Chapter 3 on the technical approach describes in the first section the working theory of the generator. This chapter begins with the ideal equations which make the foundation of the operation of the spiral generator. Equations to determine the electrical characteristics are presented followed by discussion of their importance and relevance. The most important of these, the output capacitance and inductance, have several methods presented which have different use cases. Inductance is one of the more focused upon characteristics and most methods described can be found in the text of Grover on inductance calculations [8]. Finally, modeling considerations are presented including two equivalent circuit models. Three models are discussed including the one used in this work which was a simple sinusoidal equation for the output waveform. The section on materials describes the insulator and conductor materials used in the fabrication of the spiral generators, switches used, the sensing apparatus used, and the designed winding apparatus. It briefly describes

any other miscellaneous material or equipment used. Some discussion on recommendations for material is also found here. This is followed by the approach taken in detail.

Then in Chapter 4 results are introduced for both the initial tests and the comparison of the model. This begins with results of the initial tests to provide a simple overview of a single spiral generator. These results are compared with those of the simple time-dependent model in addition to the results from other works. Some brief discussion of these results and trends specific to each set of results can be found in this Chapter but final conclusions and common trends are left for Chapter 5. In addition, the time-dependent model developed is compared to the geometric study performed by Yan *et al* for comparison with more experimental data and the model utilized in that paper [7].

Finally, Chapter 5 discusses the significance of the results. The problems overcome or otherwise avoided over the course of the research are discussed in detail there. These problems include switch bounce, trimming of the output voltage by the ratio of output capacitance and the load capacitance, and the problems regarding the development of a more accurate model. Switch bounce refers to a phenomenon of intermittent connection in physical switches caused by the contacts bouncing off one another repeatedly. In addition, discussion on more consistent and higher quality fabrication methods for spiral generators are discussed. Trends common to both experimental and modelled results are noted here, followed by discussion of their relevance. The limitations of the model developed and discussions on the proper use of the model are also discussed here, as well as possible future work to improve the model while maintaining its simplicity.

Chapter 2. Literature Survey

2.1 Works Pertaining to Spiral Generators

This section of the literature survey refers to spiral generators alone. This is done to distinguish the spiral generator from other vector inversion generators covered later in the literature review.

2.1.1 The 1964 Presentation of the Spiral Generator by R. Fitch and V. Howell

The spiral generator entered the field of pulsed-power as an invention of R. Fitch and V. Howell in 1964 [4]. The stated objectives are to show how voltage multiplication can be achieved using transient reversal of voltages in series connected systems. A pulse generator that utilizes this method is called a vector inversion generator (VIG). The effort sets out to present three types of generators utilizing this method, and one of these generators is the spiral generator. The document begins with the operating principle of a vector inversion generator. The spiral generator is stated to be a form of a stacked transmission-line vector inversion generator. Shown alongside the stacked transmission-line generators is lumped circuit generators such as a Marx bank or LC generator.

Fitch and Howell begin to go into more detail by introducing the governing equations for the stacked transmission-line generator with an emphasis on the spiral generator variant of the stacked transmission-line generator. This is where some of the key equations used in this study are introduced in their original form, some of which like the simple output voltage equation remain unchanged. One interesting note that remains unseen in other research is that coaxial lines may be used but have different behavior due to usually having higher impedance than strip lines.

2.1.2 The 1976 Work of A. Ramrus, and F. Rose on Spiral Generators

One of the first notable contributions is the beginning of the work of A. Ramrus and F. Rose starting in 1976 [5]. This study was performed by A. Ramrus and F. Rose in which spiral generators explored at high output voltages up to 1 MV. The generators studied had relatively low efficiencies of 0.3 to 0.5. The methods used focus on the fabrication and experimental testing of spiral generators. Insulation used varied between air, oil, mylar, and other solid dielectrics. The knowledge and use of low inductance switches such as solid-dielectric or rail gap switches shows a basic knowledge of switching effects even this early. Many of the generator failures experienced by Ramrus and Rose were caused by breakdown at the edges of the conductor before triggering. They suggest this points to the breakdown caused by the DC charging voltage and can be remedied by grading the field at the edge of the conductor.

The primary method used in A. Ramrus and F. Rose's exploration of spiral generators was simply to fabricate and operate these generators. They utilized several different configurations and modifications on their generators depending on the objective. In the original publication, they experienced generator failure due to breakdown during charging. Noting the cause to be the electric fields at the edges of the conductors, Ramrus and Rose utilized resistive paper applied to the edges to grade the electric field there. Additionally, in order to get the desired high-voltage output they would need significant insulation between the conductors. This insulation came in the form of air, which had been the insulator of choice in previous efforts, plastic insulation such as mylar, and eventually castor oil impregnation. The switching methods used trended towards solid dielectric

switches, which could be set by varying the thickness of the mylar used. This was likely done due to the lack of three electrode rail gap switches at the time.

The failures at the conductor edge led to the conclusion that grading the electric field at the edge could increase allowable charging voltage. They also conclude as many will later that the L/Z ratio of the operating switching must be around a tenth of the double transit time of the generator. This ratio is later used to explain the switching efficiency factor of the total multiplication efficiency of the spiral generator, and is one of the most common mistakes made to result in a lower than 50% multiplication efficiency.

2.1.3 The 1980 Work of F. Rühl and G. Herziger on Modeling Spiral Generator Behavior

Work on a more exact model of the behavior of the spiral generator is published in 1980 by F. Rühl and G. Herziger [9]. This model is a lossy model and is briefly compared to the lossless or ideal model of a spiral generator. Other than the model some effects such as that of differing switch potentially resulting in a doubled output voltage are noted. The relationship of switch rise time to the rise time of the generator and capacitive loading of the generator are also noted. They briefly relate the behavior of the spiral generator to certain configurations of a spiral pulse forming line as an end to the publication.

For the model of the behavior of a spiral generator the generator was modeled as two stacked striplines shunted by the attached load and the internal inductance of the generator. Using Laplace transforms they get an equation for the normalized output voltage in the Laplace domain but notably do this by eliminating the input switch current. They were able to consider capacitive loading, and more interestingly the effect of the stray capacitance by treating it as a capacitive load.

The model produced by Rühl and Herziger was a good foundation for future modelling work on the behavior of the spiral generator. The model is accurate enough to be utilized at least over the the first two peaks, which are often the most important to utilizing a spiral generator in a system. Rühl and Herziger notes that the stray capacitance found within the windings, as well as the input and output terminals of a spiral generator can have a significant impact on the output voltage. This is especially true for spirals storing less energy. While noting the impact of the rise time of the switch on the rise time of the generator and its operating efficiency, Rühl and Herziger conclude that the impact is less than 15% so long as the ringing frequency is smaller than that of a maximum defined by geometric and dielectric properties. Of particular interest is the conclusion that placing the operating switch into the middle of the active line rather than the edges can more than double the output voltage of the generator. It is however noted that this is only true if the switching characteristics and rise time of the generator have been chosen accordingly.

2.1.4 The 2005 Continuation of the Work of Ramrus and Rose by F. Rose, Z. Shotts, and Z. Robert

The work of Ramrus and Rose is continued starting in 2005 by Rose with the help of Z. Shotts and Z. Robert [10]. Here a deconvoluted equivalent circuit along with the relevant equations derived from it are presented. These equations allow for the modelling of the amplitude and times of the output waveform independent of charging voltages, efficiencies, or losses. This can be applied to the simplest equation for output voltage to yield an approximation of the output voltage waveform. The result matched well with their experimental results but disagreed with the conclusions of J. Yan and S. Parker *et al* made

in 2021 that equivalent circuit models cannot compensate for the effects of wave propagation when predicting the output waveform [7].

In the design principles put forward by Z. Shotts, Z. Roberts, and F. Rose the generator is explained by a series of basic design equations. These equations describe primarily the electrical characteristics of the generator or the energy relationships. In this effort, the effects of different insulator and conductors are mentioned in their relevancy. It is noted that Teflon would be a prime choice if not for difficulties caused during fabrication by the physical properties of the insulator. It was noted that in the construction of spiral generators for testing that it was of utmost importance that quality windings was assured. In order to achieve this a winding machine similar to that used in capacitor fabrication was designed. This machine however could take a much larger range of material widths and winding mandrels with a variety of thicknesses. The winding machine was touted as invaluable to the research and should be considered in any research involving fabricating spiral generators.

The design principles by Z. Shotts *et al* show that the spiral generator can be designed for a large variety of applications while being space and cost effective. It is noted that they are rather simple theoretically but the associated variables with them are more complex. In closing it is stated that the previously unknown intricacies of the spiral generator are being explored towards achieving a more proven design.

2.1.5 The 2007 Efforts of E. Pal'chikov, E. Bichenkov and Associates Towards the Refinement of the Theoretical Model of the Spiral Generator

In 2007-2011 Bichenkov, Palchikov, and associates presented a multiple refined versions of the original model proposed by Fitch and Howell when the generators were

invented in 1964 [11]–[13]. They noted the modeling work of Rühl and Herziger with the conclusion that while many of their equations were presented incorrectly written that the final equations were correct. Additionally presented is the slightly modified Belkin Zharkova model for the Tesla transformer which turned out to be much more accurate to the behavior than the model of Rühl and Herziger.

Deriving the model from charge conservation equations and drastic modifications to the model of Rühl and Herziger, the model was made into a dimensionless form. This final form was a system of four partial differential equations with rather complex boundary conditions. Due to the use of conservation laws, this model was solved using Godunov's method. A second model was also presented by modelling the generator as if it were a tesla transformer using a model provided by Belkin and Zharkova. It is found with this model that despite the disregard for wave travel the conservation laws remain valid in integral form, and that the voltages and currents remain as smooth as that from a simple tesla transformer.

It was concluded that this model was more accurate for generators with many turns. For a small number of turns they note that the generator can likely be modeled as a lumped capacitor. For the Belkin and Zharkova model it was observed that the model itself casts doubt on the validity of Fitch's original model of a spiral generator as well as the model of Rühl and Herziger. A final conclusion that is important is that spiral generators with many turns will suffer from a decrease in efficiency as the number of turns increases. This modeling was later used to develop a spiral generator to be used as a supply for a pulsed-power device to drive an X-ray generator which was developed and utilized afterward.

2.1.6 The 2007 Continuation of the Work of Schotts and Rose with the Contributions of J. Hanlon

In 2007 J. Hanlon worked with Z. Shotts and M. Rose to continue their megavolt scale research on these generators [14]. In this effort triggering of spiral generators with solid-state methods was explored. This was driven by a better knowledge of the high currents and current derivative requirements, the solid-state switch technology, and a better understanding of the spiral generator itself. This would be the beginning of an effort to use spiral generators to make increasingly compact solid-state switched trigger systems. Synchronously Shotts and Rose continued their work with Z. Roberts in order to explore the design of spiral generators. Due to the still poorly understood behavior of the spiral generator at the time the effort took up the objective of providing a set of design principles. The goal being that if followed the principles would yield a generator design which fell within a few percent of theoretical values. In this work equations are presented to allow determination of energy available from the spiral generator, charging time, and load impedance requirements. These design principles were demonstrated by design and operation, and discussion of applications was also performed.

The desire to simply operate the spiral generator using more reliable switches lead to the utilization of solid-state switches. These switches had better repetition rates, were easier to trigger, and do not need pressurized gas or maintenance of electrodes. In order to explore this, testing was performed with a thyristor. This allowed the exploration of the effects of a solid-state switch on the behavior of the generator with the goal of eventually finding a failure mode. Due to the nature of these solid-state switches protection from back-current was required as well as a trigger control system. This required anti-parallel power

rectifier and some other trigger system protections on the gate. In addition, in order to prevent charging current from holding the thyristor closed a digital delay generator was used to force the power supply used into shutdown mode. The combination of these protections and the control system was enough to allow ease of repeatable testing with only a singular button.

These results revealed some important initial findings. Notably the negative voltage swing from the operation of the spiral generator caused a large negative current to flow back to the gate of the thyristor. Considering this current was important as it could damage the thyristor during operation, and with protections added no failure occurred during their testing. Comparison of the operation of a spiral generator with a spark gap switch compared to that of a solid-state switch shows that the repetition rate is limited by the slower rise time. This slower rise time is caused by the current limiting resistor. In addition, these switches were noted to switch and conduct over a large range of voltages. This range was found to be wider at higher rep-rates and while it could be remedied the problem is not present in solid-state switches. The solid-state switches were found to be a simpler and more elegant solution overall.

2.1.7 The 2021 Exploration of Switch Characteristics and Modeling of Loading Effects by J. Yan, S. Parker, and Associates

More recently in 2021, J. Yan and S. Parker explored the function of spiral generators with a focus on switch characteristics, the modification of a Palchikov's model to account for load effects, and the use of the generators to operate spark gap switches in extremely compact forms [7], [15]. This took the form of two separate journals and in the first the effects of switch characteristics on the behavior of the spiral generator were

explored using thyristor switches. These solid-state switches were chosen for their low inductance and placed in parallel to reduce inductance and current stress on the switches. This exploration included the theory of operation for a spiral generator, the effects of geometry on output characteristics, and the addition of load effects for different loads. In the second exploration a spiral generator was fabricated with the objective of exploring the device as a triggering system for large scale pulsed-power systems. This generator was extremely compact with an extremely short rise time in the tens of nanoseconds and a nanosecond scale jitter.

Yan and associates first approach the problem of fabricating and testing spiral generators using common methods. A foundation for research is established using equivalent circuit model. They diverge in their methodology by first noting that few models of these generator previously are accurate for generators with many turns. Yan notes that the original phenomenological approach by Fitch and Howell are incapable of predicting the efficiency or complex oscillatory waveforms output by the spiral generator. With Fitch and Howells methodology only predicting the first pulse, it is noted that the subsequent peaks can often be more useful than the first. To remedy this, Yan et al utilizes the model of Pal'chikov *et al* to describe the behavior of the generator with different switching characteristics. This model is later modified to account for load effects. A generator was constructed for testing using mylar insulation and copper foil as the conductor. The effects of switch inductance are explored by testing at extremes with very low inductances. To achieve this inductance Yan et al utilizes thyristor switches in parallel as the input switch. These solid-state switches are chosen primarily to avoid the disadvantages of miniature triggered spark gap switches. Some problems were found in using solid-state switches as

they would often show little improvement in multiplication efficiency in addition to sustaining major damage during operation. The SP-205 solidtron switches used were a recent technological development which had improved current uniformity. In order to trigger these switches simultaneously the gates were connected to four uniform secondaries of a transformer.

Later when this research is expanded a similar switching system is used in which the results from the original research are leveraged to allow more compact design. The generator used again uses mylar and copper foil and is housed in an ABS plastic case. The load selected was a Kovalchuk ball switch. It was found that the mylar insulation had to be quite wide compared to the conductor width to prevent breakdown at the edges. Two switching methods were used. These were the solid-state thyristors from the previous effort, and a miniature triggered spark gap. One of the considerations stated for switching was that solid-state switches such as MOSFETs or SCRs had much too low of a rise time or slew rate in order to properly operate the generator. In order to enhance the output of the generator tested for use in triggering a pulse sharpening output gap was used. This spark gap not only sharpened the rising edge of the output pulse but was designed to be polarity dependent such that it would trigger on the second higher amplitude peak of the spiral generator. This polarity dependence can be used as the second peak was of opposite sign to the first. Three generators were tested experimentally in which the only difference was switching method. One with four thyristors, one with six thyristors, and one with a miniature triggered spark gap.

In the two journals published by Yan and Parker, several sets of results were presented. In the first effort results of the effects of geometrical, switching, and load

characteristics on the behavior of the spiral generator were explored both computationally and experimentally. The results of the computational model were generally accurate within 10%. All results were presented in a normalized time and voltage relative to the transit time of the generator and the charging voltage respectively. It is noted that despite the output capacitance and inductance of the spiral generator being increased an order of magnitude the oscillatory period of the output remained mostly the same. This is evidence that suggests the wave propagation is the dominant component of the period of the generator. Yan and Parker note that it is likely that equivalent circuit models alone will thus fail to predict the structure of the output waveform. For the simulated results agreement was strong for the first few periods but diverges from experimental results as time progresses. Notably this effect becomes more pronounced as the number of turns on the generator decreases. The effects of resistive loads are relatively unchanged for loads greater than 50k Ω . For resistances lower than this the amplitudes of the peaks are reduced as the resistance decreases while the period remains unchanged. Capacitor loads increase the oscillation period while simultaneously decreasing the output amplitude as the load capacitance increases. The load inductance increases the oscillation period is increased. To close, considerations on producing pulses for various applications were discussed.

In the second work, the results for the generator driven by the spark gap are presented first. This generator sees a relatively low efficiency of 19% with a multiplication factor of 9.3. A large second peak is noted with an multiplication factor of 13.3. It was noted that this larger secondary peak is common of many spiral generators but its cause is not very well explored. Yan and Parker note that the theory suggests the existence of this peak may be dependent on whether the load driven is capacitive or resistive. The

experiments with the six thyristor configuration show a better initial efficiency with a multiplication factor of 12.7 and the four thyristor configuration resulted in a multiplication factor of 10.2 but was capable of a secondary output peak with a factor of 13.9. This is a good example of the difference of switching effects on the behavior of the generator. Of the different generators used all had rise times under 100ns and all had jitter less than 10 ns and as low as 2 ns. This jitter was noted to remain constant regardless of the charging voltage. Yan and Parker found that the results from the two different thyristor versions suggested that the resistance of the switch varies depending on the voltage applied at the gate for triggering.

2.1.8 The 2022 Exploration of Liquid Dielectric Use in Spiral Generators by Isaac Cohen and Associates

Another recent study which diverged in methodology and approach from many of the previous works was that of I. Cohen *et al* where the insulation of the spiral generator was replaced with only liquid dielectrics [6]. This effort was also overseen by Radiance Technologies like the works of Rose and Shotts previously. The use of liquid dielectrics was found to be desirable due to the need for a regenerative dielectric as the spiral generator often fails from dielectric breakdown at high-voltage inputs. This study was performed with the goal of evaluating manufacturing methods compatible with liquid dielectrics, the self-healing capabilities of the liquid dielectrics, and the viability of the designs.

The use of liquid dielectrics saw Cohen and associates approach fabrication in a different manner than the winding methods in other works. Rather than winding the primary method employed the conductors were rigid and fabricated using three methods. This was required due to the lack of structure normally provided by the tight winding and

solid insulator. The three manufacturing methods were direct metal laser sintering, 3D printed parts, and wire electrical discharge machining. The last of the mentioned methods was said to have the best results. Of final note, is the presentation of a more accurate method for calculating the inductance of the spiral generator, and the mention of the two operational frequencies.

Testing revealed the best results from the wire electrical discharge machined spiral generators. The most notable results were that even in the event of breakdown that the spiral generator would remain functional and in fact had negligible damage to the conductors. Cohen notes that the output capacitance remains a difficult parameter to determine solely through calculation. The future open challenges to this configuration of a spiral generator is stated by the authors as being the demonstration of output voltages in excess of 300 kV to demonstrate extended lifetimes, demonstration of enhancement using magnetic materials, improvements in the determination of the resonant frequency of the spiral generator, and a more thorough and understood circuit model to improve simulations of the generator.

2.2 Works Pertaining to Other Vector-Inversion-Generators

This section covers other explorations into vector inversion generators as these are significant to the function of the spiral generator. This is because they use the same basic principle of operation as the spiral generator does. They do, however, apply this basic principle using different methods.

2.2.1 The 1971 Exploration of Marx Generators by R. Fitch at Maxwell Laboratories

Marx generators have taken a strong position in pulsed-power systems since their invention in 1924 [4]. These generators saw a major research and development effort at Maxwell Laboratories overseen by R. Fitch in 1971 [16]. In this effort, Fitch explores switching considerations involving a change in direction from the simple 2-electrode spark gap to a 3-electrode switch also called a rail gap switch or solid dielectric switches. Fitch notes the geometry used to sustain high-voltage over long times was generally done using open geometries which added to the inductance and thus the rise-time and peak power of the generators. A proposed geometry can be seen in Fig. 3 to reduce this effect. Fitch describes the advantages and disadvantages of different configurations of Marx generators including Erwin Marxes, Martin Marxes, and their new configuration the aptly named Maxwell Marx.

In Fitch's original exploration of Marx banks, he notes that most of the geometrical constraints involving Marx generators is caused by the thickness of capacitors rather than for protection against arcing. In this exploration, Fitch notes the use of two electrode switches, and instead presents a three-electrode design. This switch is triggered by applying high voltage to the additional electrode which then arcs to the two original electrodes common to these switches. This is different from the two-electrode version as in that configuration the switch is triggered by direct breakdown between the electrodes. This three-electrode configuration was explored primarily to increase the factor of safety involving pre-fires. Most of the methodology utilized by Fitch involves experimentation with different switching and triggering methods such as his development of a Marx control

system and the three-electrode switch. There is also a heavy focus in this effort on the geometry and its effects on the inductances and self-capacitances of a Marx generator.

2.2.2 The 2003 Exploration of Switching Methods for Marx Generators by K. LeChien and J. Gahl

In 2003, K. LeChien and J. Gahl explored switch design for Marx banks [17]. This is because the Marx bank usually has a high inductance and requires frequent maintenance. In this effort, they sought to define arcing behavior in spark gap switches. This was specifically to design multi-channel switches. The multi-channel switch reduces inductance due to parallel channels and also distributes the erosion caused by the arcing to result in less maintenance. K. LeChien and J. Gahl used a triggered and pressurized spark gap to determine experimentally the impact of different characteristics on the number of channels formed in a multi-channel switch. These characteristics are namely pressure, gas type, charge voltage, and the trigger voltage amplitude and waveform. In order to determine the number of channels formed, a high-speed camera was used. It was determined that many channels should result in a lower switching inductance, and by calculating the ringing of the output current they were able to confirm that this was the case. They admit that while there is no clear correlation between the number of channels formed and the effects is obtained, that this will reduce electrode erosion. They point out that with the inductance having a high error and lack of consistency due to inconsistencies in channel formation, that this form of switch should not be used with the intention of reducing switching inductance of a Marx bank

2.2.3 The 2011 Effort on Improving the Efficiency of the Marx Generator by N. Mutnitskii and V. Tatur

N. G. Mutnitskii and V. V. Tatur explored methods in order to improve the output voltage and inversion efficiency of a Marx generator in 2011 [18]. In this exploration the objective was to increase the factor of voltage multiplication without increasing the number of stages required. This was a successful endeavor in which a modified Marx generator is presented which has a significantly higher output voltage than an ideal generator. The circuit of the resulting system of this effort can be seen in Fig. 4 below.

In order to reach the increased voltage output desired in their 2011 work, N. Mutnitskii et al developed an alternative way for controlling the charging of the capacitors in a Marx generator. The use of controllable diodes and inductors rather than charging resistors allowed the generator to reach operating voltage much faster. It was found that in this configuration that the generator would oscillate and by precisely controlling when the diodes allowed current to pass the generator would ideally be able to output double the voltage amplitude it would normally. The oscillation that makes this possible is caused by the LC circuits within the generator and place this configuration into a gray area where it is not quite a Marx nor an LC generator. The results from this effort show an alternative configuration for the Marx generator capable of outputting double the ideal output voltage expected. This is an oscillatory output which takes the form of very sharp, negative and uniform pulses. As with most VIGs this output voltage is programmable and can be designed to a repetition rate. In the case of this work the repetition rate was 10 kHz.

2.2.4 The 2000 Exploration of the Transformer-Coupled LC Generator by T. Engel and Associates

In 2000 T.G. Engel et al explored a variation of the LC vector-inversion-generator called a transformer-coupled LC generator [19]. This generator while similar to a Marx generator has the added benefit of requiring only one operating switch rather than one every other stage like the LC generator. The circuit diagram of this configuration can be seen in Fig. 5. This is noted as having the disadvantage of increasing size and weight of the generator as the switches are replaced by usually larger and heavier transformers. In this effort the equations regarding the operation and behavior of a transformer coupled LC generator are presented.

In order to model the behavior of the transformer coupled LC generator, Engel derives equations for the voltage across the capacitors in an LC generator stage. This is done in the frequency domain which resides in the Laplace domain. These equations allowed Engel to show the problems of efficiency with increasing stage number numerically. It is noted that multi-stage transformer coupled LC generators are difficult to analytically model. In order to illustrate the modelling equations presented, the team of Engel experimentally tested many of these generators. Consistency of the properties of the transformer cores are considered critical to agreement between the experimental and modeled results. The core must also be properly sized to prevent saturation. It is also important that the transformer, which must be a 1:1 ratio, have a very high coupling coefficient for efficient operation. It is ideal to have a coupling coefficient greater than 95%.

Engel finds that the transformer coupled LC generator can be modeled with reasonable accuracy should the parameters of the transformers used be well known. He notes that the use of a single switch brings greater reliability at the cost of inversion efficiency. While the transformer coupled LC generator charges much faster than a Marx generator, and requires less maintenance, it suffers from a larger scale, and weight. A final comment made by Engel states that problems of scaling become more apparent at higher energy levels as the cores of the transformers used must be larger to prevent saturation.

2.2.5 The 2020 Exploration of an Alternatively Configured Transformer-Coupled LC Generator by R. Bischoff

In 2020 R. Bischoff explored a transformer coupled LC generator which utilizes transformers in a parallel configuration instead of in series [20]. This causes the transformers to rise together rather than sequentially. This work builds on that by T. G. Engel previously and uses some of the equations derived in that effort. It is noted that the capacitors must be sized to compensate for the parallel rising of the transformers for the inversion to be effective. This results in the capacitors of each successive stage becoming smaller and thus limits the number of stages possible in this configuration. The configuration which can be seen in Fig. 6 results in an overall faster rise time of the generator as a whole. This faster rise time of course causes higher stresses on the switch due to the current time derivative.

For the alternative circuitry for a transformer coupled LC generator presented by Bischoff to be successful a few requirements were defined. The first requirement is a transformer with a coupling coefficient as close to unitary as possible. Another requirement is related to that of the insulation of the windings of the transformers, as the operation of

the LC generator causes voltage drops across the primary and secondary windings. Knowledge of the operation of the LC generator allows an equation for the required voltage rating of the insulated cable used to be derived. A final notable requirement to be considered is the high switch current and switch current time derivative. This is not of extreme importance for rail gap switches but should be considered for solid-state switches to prevent damage. In testing the tools of choice for Bischoff were a pressurized gas switch, ceramic disk capacitors, and a custom fabricated transformer with bifilar windings.

Bischoff notes that the results of their alternative circuitry shows a faster rise-time of the output voltage as expected, but also confirms the problems of increased switching currents. As expected, there is no difference in output between the single-stage configuration and the output of a normally configured transformer coupled LC generator. This is because there is only a singular transformer so no difference in connection between transformers can be established. The capacitor compensation required for the configuration to operate was found to produce a higher risetime than expected. A final comment is that the no compensation methods are strictly necessary and that the design of a transformer-coupled LC generator is simpler in this configuration. Downsides such as the requirement for higher breakdown ratings in the transformer insulation, and higher switching currents should be considered but are in no way inhibitive of performance with care.

Chapter 3. Methodology

3.1 Investigation

In this section the working principles of the spiral generator are discussed in more detail. Models and equations that describe the behavior of the spiral generator are presented here.

3.1.1 The Idealized Spiral Generator

A spiral generator is a type of vector inversion generator (VIG) which is composed of two conductive lines, usually metal foil or sheet. This generator is charged up to an input voltage u_0 which provides the energy for the generator to operate. This energy is stored electrostatically between the two conductors. When operated by closing a single input switch connected across the outer turns of the two conductors the generator produces a voltage multiplied pulse at the output of the inner most turn. The peak output voltage can be approximated using Equation 3.1:

$$u_{out} = -2\varepsilon_{ff}Nu_0, \quad (3.1)$$

where N is the number of turns of the generator, and V_{in} is the charging voltage.

The above output voltage is ideally a triangle wave with a rise time equal to twice the electrical length of the active line. This is far from representative of the real behavior of a spiral generator as the consideration of different losses results in a sinusoidal output voltage consisting of two frequencies. The ability to determine the shape of this output waveform has been a focus of the majority of the studies on spiral generators.

The two conductors of a spiral generator are wound around one another to form a spiral geometry with connections made on the inner and outer turns. Insulator must be

placed between the conductors with a dielectric strength capable of withstanding twice the charging voltage. This geometry effectively forms two capacitive lines from three electrodes which are referred to as the active and passive layer [21]. An example geometry can be found in Figure 3.1 which depicts the passive conductor in red and the active conductor in black. This is a common geometry but not the only one used. Some configurations include additional outer or inner turns. Others may see the switch and load swapped. This simple geometry among other factors has seen the spiral generator become a favorite for extremely compact trigger generators [15], [22], [23].

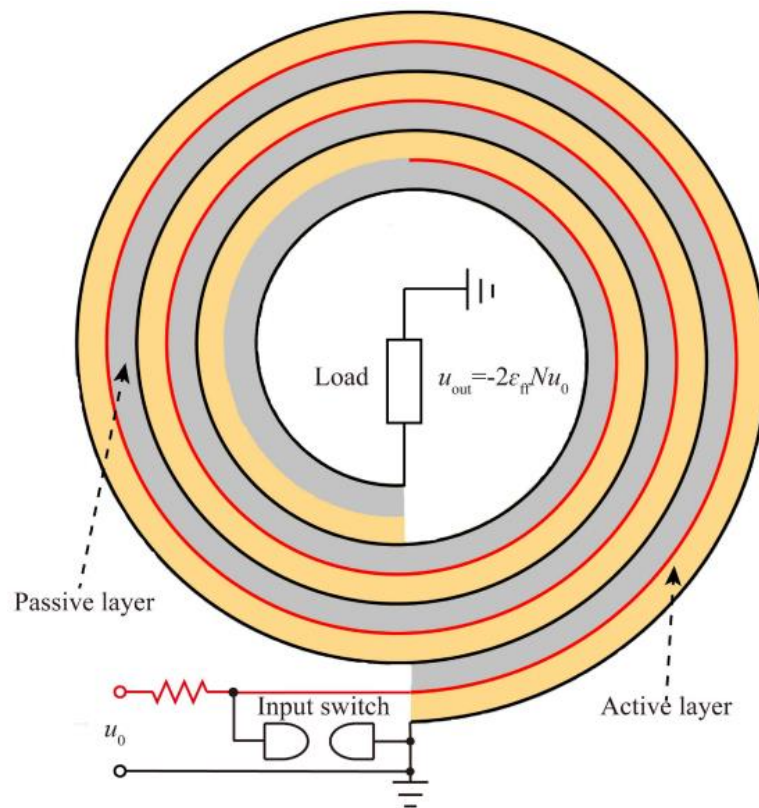


Figure 3.1 Example Configuration of a Spiral Generator [7].

Like all VIGs this generator functions by inversion of electromagnetic vectors during the pulse forming process [21]. This process starts when the input switch is closed at time $t = 0$. Before the switch is closed the voltage at the output is either electrically

neutral such as in this case or at the charge voltage depending on geometry [24]. When the switch closes a pulse travels down the active conductor towards the load. As this wave travels it converts the electrostatic field between the two conductors of the active layer into an electromagnetic field [4]. When this pulse reaches the output end at $t = T/2$ it reflects and begins to travel back towards the switch. At this instant the vector inversion begins. This re-establishes the electrostatic field as the wave travels with the field inverted in direction towards the center of the generator. An internal view of the electrostatic fields before and after the wave reflects can be seen in Figure 3.2.

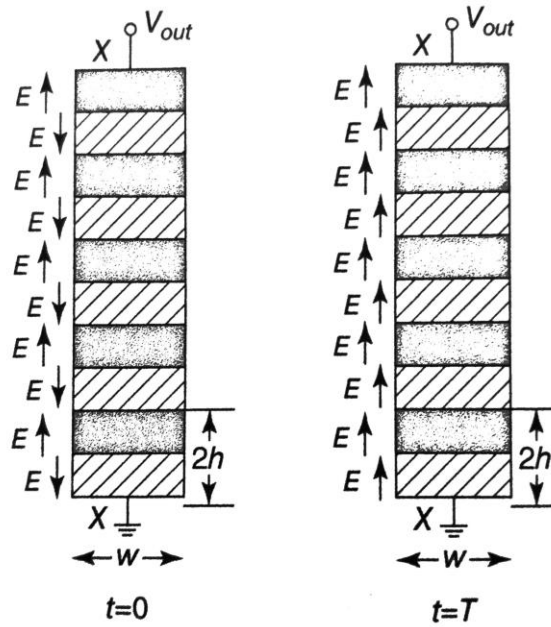


Figure 3.2 Internal example of vector inversion [7].

The generator ideally reaches the maximum output u_{output} when the wave has returned to the switch because the electrostatic fields concentrate at the center of the generator where the output is. The time to reach the maximum output is twice the electrical length of the active conductor. This can also be calculated using the effective wave velocity inside the active layer using Equation 3.2 and Equation 3.3:

$$c_{eff} = c/\sqrt{\epsilon_r\mu_r}, \quad (3.2)$$

where c is the speed of light, ϵ_r is the relative permittivity of the conductor, and μ_r is the relative permeability of the insulating layer material. Then Equation 3.3 yields the period:

$$T = 2L/c_{eff}, \quad (3.3)$$

where T is the time for the generator to reach the ideal max output, L is the length of the conductor, and c_{eff} is the effective wave velocity from Equation 3.3.

After this time the wave will continue to reflect over the same timescale, producing an oscillating output waveform which will slowly decay as the energy stored within the electrostatic fields is diminished. Ideally the output would be a triangle wave, but in practice resembles sinusoidal oscillations. This time T remain the same regardless of charging voltage or load characteristics and is a factor only of the simple geometry of the generator. This is because despite equivalent circuits portraying the generator as an LC circuit, the oscillation period is dominated by wave propagation [7].

3.1.2 Important Parameters and Electrical Characteristics

While the above theory is simple in ideal cases, the electrical and geometric characteristics of the generator interact with one another during the pulse forming process. This oversimplified, is due to the electrical nature of the wave, and the geometric nature of the field vectors. The first electrical parameter of note is the inductance of the generator's turns L_N which can be calculated using the formula for a winding coil in Equation 3.4:

$$L_N = K' \frac{\mu_r\mu_0\pi D^2 N^2}{2w}, \quad (3.4)$$

where μ_r and μ_0 are the relative and vacuum permeability respectively, D is the inner winding diameter, N is the number of turns, and w is the width of the conductor.

K' here is determined by the geometric parameters but is usually 0.159 [7]. It can be determined from Grover's book on inductance calculations using Equation 3.5 [8]. While this was the method used by Yan *et al*, Cohen *et al* used a method more accurate for thicker generators with a low number of turns [6], [7]:

$$L_{out} = 0.001N^2r_{mean}P - 0.004\pi Nr_{mean}(G_1 + H_1), \quad (3.5)$$

where P is a function of the geometric properties of the spiral and G_1 and H_1 are correction factors also determined by the geometric properties.

Tables and equations for these can be found in Chapter 17 of F. Grover's text on inductance calculations [8]. While this is fine for the generators constructed by Cohen, a more accurate equation for generators similar to those made by Yan can be found in the same text and seen below in Equation 3.6 This equation is more accurate for coils with thinner conductors and in fact can be used for almost any configuration:

$$L_{out} = 0.019739N^2 \left(\frac{D_{mean}}{w} \right) K'. \quad (3.6)$$

This inductance is important due to the impact on the generator's performance, namely but not solely the multiplication efficiency ϵ_{ff} . This is primarily due to the inductance of the switch L_S , which should yield a rise time of 10% of the generator's transit time T for nominal efficiency [9]. The impedance of the switch should also be less than that of the active line. The reason for this is that the pulse formed when the switch closes must have a rather sharp leading edge. With the switching characteristics being important, it may be prudent to know the current and required time rate of change of current the switch must tolerate. These can be approximated using Equation 3.7 and Equation 3.8 respectively while also noting that it is assumed that $\sqrt{L_{switch}/C_{in}} > R_{switch}$ [24]:

$$I_{max} = u_0 / \sqrt{L_{switch} / C_{in}} \quad (3.7)$$

$$\left(\frac{dI}{dt}\right)_{max} = \frac{I_{max}c}{\sqrt{\epsilon_r \epsilon_0 L}}, \quad (3.8)$$

where ϵ_r and ϵ_0 are the relative and vacuum permittivity respectively of the insulator.

Another important electrical parameter to consider is the output capacitance of the generator, which should be higher than the capacitance of the load for nominal function. This capacitance cannot be measured and only exists during the pulse forming process, which is the capacitance of the two capacitive and three electrode transmission lines formed by the generator geometry. While it cannot be measured it can be calculated using Equation 3.9 from [9]:

$$C_{out} = \frac{\epsilon_r \epsilon_0 \pi D w}{2Nt}, \quad (3.9)$$

where ϵ_r and ϵ_0 are the relative and vacuum permittivity respectively of the insulator, and t is the thickness of the insulator separating the active and passive conductors.

Because there are effectively two capacitive layers during the pulse forming process, the capacitance of each layer is twice that of the output capacitance [7]. It should also be noted that the input capacitance C_{in} can be measured and used to calculate output capacitance using $C_{in} = 2N^2 C_{out}$. This equation can be easily derived from an energy balance stored in the input and output capacitances when charged to the input and output voltages seen below in Equation 3.10 [5]:

$$\frac{1}{2} C_{out} u_{out}^2 = \frac{1}{2} C_{in} u_0^2. \quad (3.10)$$

Then the output capacitance $C_{in} = 2N^2C_0$ can be derived by substituting the value of u_{out} from Equation 3.1 This is only approximate though due to not accommodating for energy losses such as those of resistive losses.

3.1.3 Efficiency of the Spiral Generator

The losses that effect efficiency can be accounted for in a simple alteration of Equation 3.1 [8]:

$$\varepsilon_{ff} = \varepsilon_1\varepsilon_2\varepsilon_3\varepsilon_4\varepsilon_5 = \frac{u_{out}}{2Nu_0}. \quad (3.11)$$

ε_{ff} consists of five efficiency factors and may be as high as 0.95 [24]. The first three of these factors are associated with ohmic losses to thermal energy with ε_1 being that of losses to the switch. ε_2 represents losses to the dielectric. ε_3 represents resistivity losses in the conductors. ε_4 represents losses due to inefficiencies of the ratio of the fast and slow conductors of the generator. ε_5 is representative of corona losses and can determine the time of total failure due to electrical arcing or dielectric failure.

Losses associated with the switch efficiency factor ε_1 result from the relationship of the switch rise time and the rise time of the generator which is roughly linear. This ε_1 is an important factor due to being able to dominate the generator efficiency and approaches zero as the ratio of generator rise time to switch rise time approaches zero. This relationship is presented by Z. Schotts *et al* seen in Figure 3.3 and it can be observed that due to this phenomenon generators with short conductor lengths are often dominated by this switching efficiency factor with other efficiency factors decreasing with length or being negligible [25]. Shorter conductors will often result in impractical switching requirements for efficient operation.

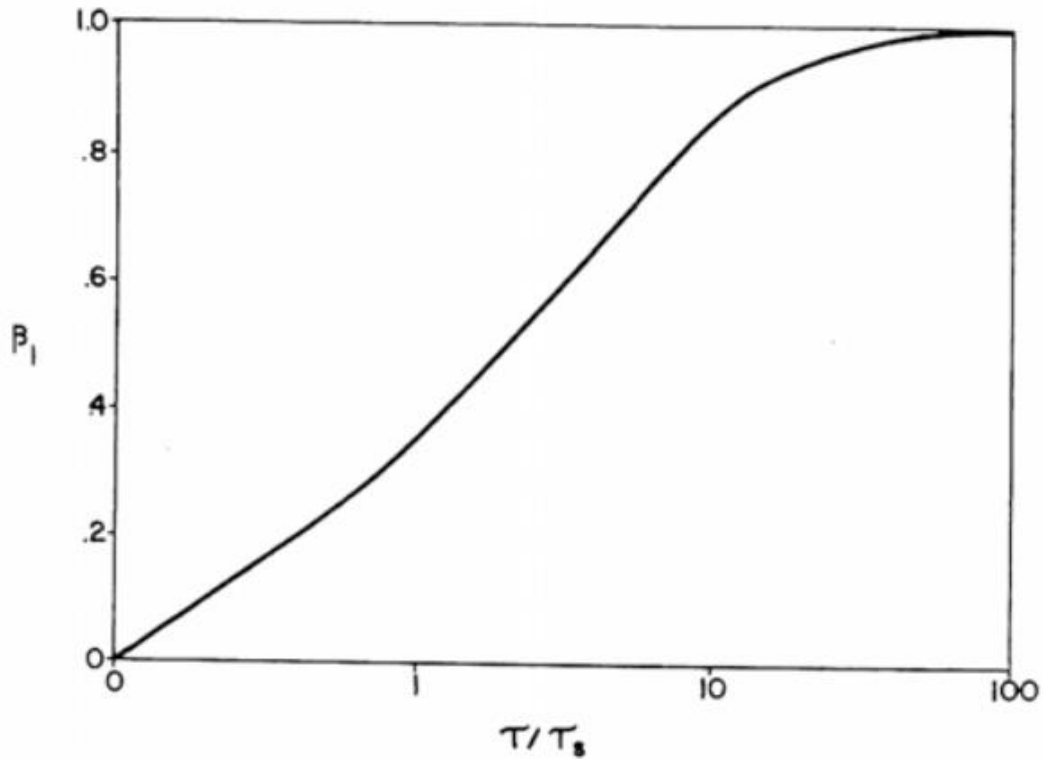


Figure 3.3 Switch rise time ratio with the first efficiency factor [24].

Corona losses represented by ε_5 are usually negligible for generators operating at voltages less than 15 kV. These losses increase due to the effective capacitance of each turn being increased by an effective increase in width of the winding due to the conducting air [5]. Sharp edges increase the electric fields generating this corona and thus conductors used should utilize smooth edges or resistive paper grading of the edges to increase this efficiency factor ε_5 in generators operating at higher charging voltages. The reduction of sharp edges or resistive grading will also decrease the propagation of streamers which will weaken the insulation layer over time and lead to failure. Both of these problems can also be effectively eliminated by utilizing generators in which the dielectric is entirely liquid due to self-healing effects and the reduction of corona due to lack of air to ionize [6].

Other than altering mechanisms having effects of the efficiencies described above the generator can be enhanced by applying external mechanisms. To increase the energy output of the generator as well as the efficiency the generator can be driven by an explosive ferroelectric generator but care must be taken when designing these for one another to ensure proper energy transfer and the survival for the spiral generator [26]–[28]. Additionally, ferrous materials may be applied directly to the generator in order to enhance the multiplication efficiency with this being especially useful for small spiral generators [10], [28], [29]. This ferrous material should also be capable of altering the frequencies the generator operates but it should be noted this will also impact efficiency [30].

3.1.4 Modeling Considerations of the Spiral Generator

The parameters and electrical characteristics mentioned previously are vital to succeed in designing a spiral generator as they allow the construction of an equivalent circuit model which has no geometric component, as it effectively simulates a single turn of the generator. Modelling the behavior in most methods are dependent on these equivalent circuits. The equivalent circuit can be found below in Figure 3.4 [7]. In Figure 3.4 the load is represented by C_L , R_L , and L_L while layers are represented by $2C_0$.

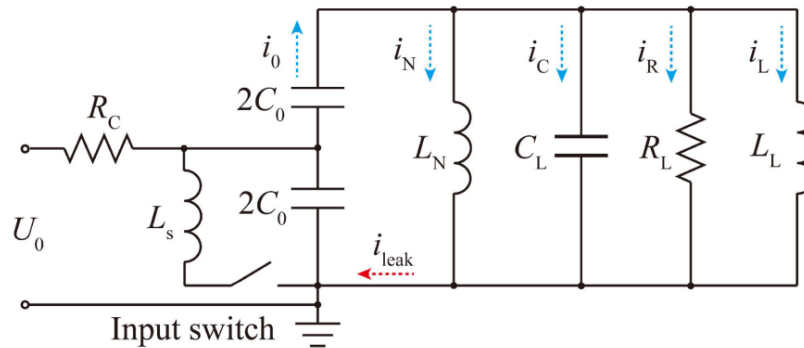


Figure 3.4 Equivalent Circuit Diagram of a Spiral Generator.

This circuit while not voltage equivalent is current equivalent if the values for the entire spiral are placed within. The charging voltage U_0 is the voltage upon entering that turn of the spiral. This equivalent circuit will not replicate the magnitude of the output voltage but using the electrical values for the entire generator will result in a similar waveform to the output waveform of the generator. Due to the lack of a geometric component, performance of the generator can be approximated with this circuit but will often fail to truly predict the output waveform's oscillatory period [7]. This is especially true with generators containing many turns [7]. While the equivalent circuit depicted in Figure 3.4 is a trivial starting point, more advanced applications will require a model to more accurately depict the behavior of a generator. The two models presented by Pal'chikov *et al* in 2012 for which one was recently utilized by Yan *et al* can provide the insight into generator behavior needed [7], [11]–[13], [15]. Despite lacking for advanced applications, the spiral generator can be carefully designed to behave close to the ideal equations described above. The work of both Yan *et al* and Pal'chikov *et al* find that these models presented do not accurately represent the behavior of generators with a small amount of turns with less than ten being a good example.

Load characteristics influence the operation of a spiral generator by effecting wave propagation as the generator operates. One of the most important of these characteristics is the load capacitance as this capacitance will lower the output voltage by lowering the multiplication efficiency ε_{ff} of the generator but otherwise is suggested to be proportional to the diameter of the conductor and inversely proportional to the length [31]. This effect is not of the same magnitude over time and has a greater effect on the second peak amplitude and subsequent peaks than it does on the first peak of the output waveform. It

should also be noted that a higher load capacitance also results in a small increase in the jitter [15]. Similarly, the load inductance results in losses due to being in parallel with the inductance of the generator. This takes the form of a leakage current i_{leak} and can impact the multiplication efficiency ε_{ff} if this inductance is too high. A final consideration on load characteristics should be that in the case of a spark gap that the rise time of the load can change the rise time of the generator. In this case if a load is connected on the opposite side of the spark gap it will also see a portion of the output voltage before the spark gap has begun to conduct [15]. These characteristics should be considered with their impact being relative to the characteristics of the generator and switch. One must be aware for small generators of stray capacitance of the windings and capacitance of the connections to the output terminals [9].

Load characteristics influence the operation of a spiral generator by effecting wave propagation as the generator operates. One of the most important of these characteristics is the load capacitance as this capacitance will lower the output voltage by lowering the multiplication efficiency ε_{ff} of the generator. This effect is not of the same magnitude over time and has a greater effect on the second peak amplitude and subsequent peaks than it does on the first peak of the output waveform. It should also be noted that a higher load capacitance also results in a small increase in the jitter [15]. Similarly, the load inductance results in losses due to being in parallel with the inductance of the generator. This takes the form of a leakage current i_{leak} and can impact the multiplication efficiency ε_{ff} if this inductance is too high. A final consideration on load characteristics should be that in the case of a spark gap that the rise time of the load can change the rise time of the generator. In this case if a load is connected on the opposite side of the spark gap it will also see a

portion of the output voltage before the spark gap has begun to conduct [15]. These characteristics should be considered with their impact being relative to the characteristics of the generator and switch. One must be aware for small generators of stray capacitance of the windings and capacitance of the connections to the output terminals [9].

While the efficiency of the spiral generator is particularly hard to model or otherwise predict, there is a promising method. The approach is to simply test a variety of spiral generator configurations at different voltages, but primarily with a range of geometric alterations. These alterations would include that of the winding diameter, number of turns, width, thicknesses of insulators and conductors, and switching characteristics or materials used. This has apparently been done before but the author has no access to this method due to the resulting model for the multiplication efficiency being proprietary due to using proprietary testing results. This does however come from a reputable source of Z. Shotts and is apparently accurate within a percent [32].

3.1.5 Modeling the Time-Dependent Behavior of the Spiral Generator

In addition to the problems with accurately determining the efficacy of a spiral generator before fabrication, the time dependent behavior and thus the shape of the output waveform can also be difficult to produce. It is known and apparent from the output waveforms observed that there are two operational frequencies of the spiral generator. These frequencies can be determined using a set of simple equations provided by Cohen *et al* [6]. These frequencies are the resonant and transit frequencies, and the first of which is produced by the oscillation of the inductance and output capacitance of the generator. While the inductance can be measured, and the output capacitance calculated from the measured input capacitance, these can be difficult to accurately surmise prior to fabrication.

The resonant frequency can be calculated using Equation 3.12 below [6]. This is usually the source of error in the time dependent behavior of a spiral generator, and care must be taken to ensure accuracy of the output capacitance and inductance:

$$f_r = \frac{1}{2\pi\sqrt{C_{out}L_{out}}} \quad (3.12)$$

The resonant frequency is calculated using the output capacitance C_{out} and the output inductance L_{out} . The latter of which can be calculated in the same way as Cohen *et al* which is found in the text on inductance calculations by F.W Grover [6], [8]. The transit frequency is simply related to the double transit time of the spiral by Equation 3.13 and is usually as accurate as the fabrication is. This transit frequency is usually more accurate than the resonant frequency and will be dominant in most generators with long conductors. For this reason, the model is more accurate in generators with long conductors as the transit frequency will make errors in the resonant frequency less apparent:

$$f_T = \frac{1}{4T}. \quad (3.13)$$

Observing that the oscillations in the output waveform are sinusoidal it is trivial to come to the following time dependent equation, Equation 3.14 for the output waveform of the spiral generator:

$$V_{out}(t) = NV_{in}\epsilon_{ff}[\cos(2\pi f_r t)e^{-\gamma_r t} - \cos(2\pi f_T t)e^{-\gamma_T t}]. \quad (3.14)$$

This equation contains most of the original output voltage equation apart from the two frequencies and the two damping factors γ_r , and γ_T . These two damping factors are only as important as the importance of the amplitude of the late time behavior of the

generator. It is notable that this equation does not account for loading effects such as that from a capacitance load or that from a pulse sharpener.

There are three additional methods that the author would like to note. The first of these methods is that of Rose and Shotts which presented the equivalent circuit in Figure 3.5[10].

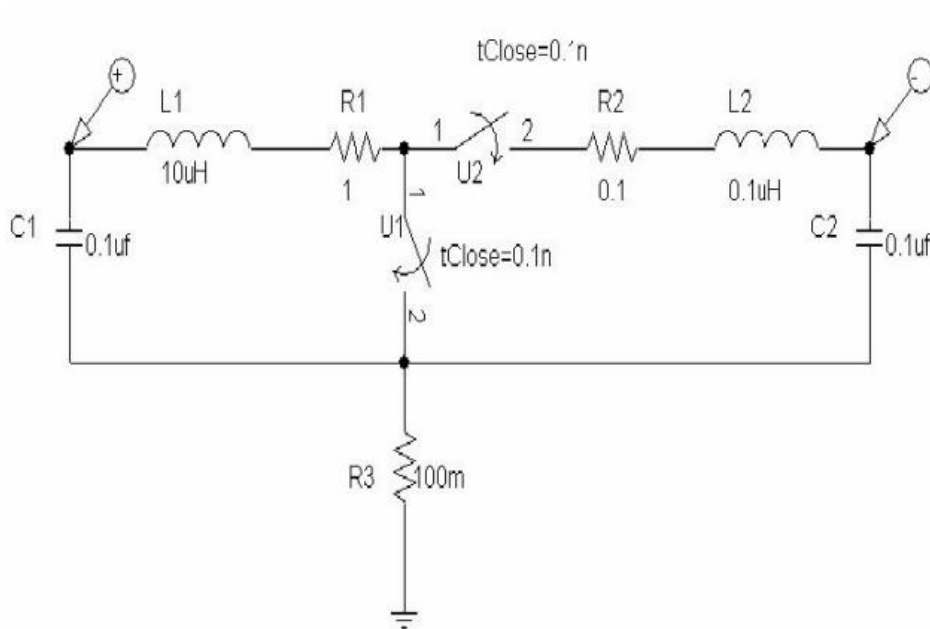


Figure 3.5 Equivalent Circuit Diagram Used by Rose and Shotts [10].

From this circuit they derived the following simple model which should look very similar to the above model. The model consists of the primary equation seen after in Equation 3.15:

$$V_{out} = V_{in} [\cos(\omega_s t) e^{-\alpha t} - \cos(\omega_f t) e^{-\gamma t}], \quad (3.15)$$

where α and γ are the damping factors of the slow and fast sides of the circuit, with ω_s and ω_f being the ringing frequencies of their respective sides of the circuit. These frequencies can be calculated using Equation 3.16 and Equation 3.17 below:

$$\omega_s = \frac{1}{\sqrt{L_1 C_1}} \quad (3.16)$$

$$\omega_f = \frac{1}{\sqrt{L_2 C_2}}. \quad (3.17)$$

The second of which is that utilized by Pal'chikov *et al* and originally developed by Belkin and Zharkova for a tesla transformer [11], [33]. The result of this is a waveform similar to the above two models, and can be found below in Equation 3.18 and Equation 3.19:

$$-U_1 = L_1 C_1 \frac{d^2 U_1}{dt^2} + M C_2 \frac{d^2 U_2}{dt^2} + R_1 C_1 \frac{dU_1}{dt} \quad (3.18)$$

$$-U_2 = M C_1 \frac{d^2 U_1}{dt^2} + L_2 C_2 \frac{d^2 U_2}{dt^2} + R_2 C_2 \frac{dU_2}{dt}. \quad (3.19)$$

The boundary conditions for Equation 3.18 and Equation 3.19 are found below in Equation 3.20 through Equation 3.23:

$$U_1|_{t=0} = U_{10} \quad (3.20)$$

$$-U_2|_{t=0} = 0 \quad (3.21)$$

$$\frac{dU_1}{dt}|_{t=0} = 0 \quad (3.22)$$

$$\frac{dU_2}{dt} \Big|_{t=0} = 0. \quad (3.23)$$

These can be solved using Runge-Kutta methods. It is determined that this tesla transformer model describes best the behavior of a spiral generator when the number of turns is small and the switch inductance is high. This contrasts with the other models which generally become less accurate for smaller generators.

The final method of note utilized by Pal'chikov et al , and Yan et al, is a modified version of a model for the spiral generator developed by Ruhl and Herziger [7], [9], [11], [15]. This is by far the most robust model in terms of load effects on wave propagation. This model will however require more development before it can be useful compared to simpler models due to its complexity. The governing equations can be found below from Equation 3.24 to Equation 3.27. Figure 3.4 is the equivalent circuit model from which the non-geometric dependent behavior is derived. Notably this allows current and switch boundary conditions to be derived:

$$\frac{\partial u_a}{dx} = -\frac{\partial i_a}{dt} - \frac{2c_{eff}N^2R_0C_0}{l}i_a \quad (3.24)$$

$$\frac{\partial i_a}{dx} = -\frac{\partial u_a}{dt} - Ni_{leak} \quad (3.25)$$

$$\frac{\partial u_p}{dx} = -\frac{\partial i_p}{dt} - \frac{2c_{eff}N^2R_0C_0}{l}i_p \quad (3.26)$$

$$\frac{\partial i_p}{\partial x} = -\frac{\partial u_p}{\partial t} - Ni_{leak}. \quad (3.27)$$

The leakage current is assumed to be constant along the length of the conductors, such that Equation 3.28 emerges:

$$\frac{\partial i_{leak}}{\partial x} = 0. \quad (3.28)$$

This is a dimensionless model such that the assumptions found in Equation 3.29 are made:

$$X = lx, \quad T = \frac{l}{c_{eff}}t, \quad U = u_0u, \quad I = c_{eff}C'u_0i. \quad (3.29)$$

The boundary conditions at the input are as follows from Equation 3.30 through Equation 3.32:

$$N^2 \frac{di_N}{dt} + k_{sa}Nn \frac{di_{0a}}{dt} - k_{sp}N(n+1) \frac{di_{0p}}{dt} = \frac{\omega_0^2}{2}u_s \quad (3.30)$$

$$\begin{aligned} -(L_z + n^2) \frac{di_{0a}}{dt} + (L_z + k_{ap}n(n+1)) \frac{di_{0p}}{dt} - k_{sa}Nn \frac{di_N}{dt} + \frac{R_s l}{L_0 c} i_{0a} \\ = \frac{\omega_0^2}{2} u_{0a} \end{aligned} \quad (3.31)$$

$$\begin{aligned} (L_z + k_{ap}n(n+1)) \frac{di_{0a}}{dt} - (L_z + (n+1)^2) \frac{di_{0p}}{dt} + k_{sp}N(n+1) \frac{di_N}{dt} \\ + \frac{R_s l}{L_0 c} i_{0p} = \frac{\omega_0^2}{2} u_{0p}. \end{aligned} \quad (3.32)$$

Some of the values in these boundary conditions are determined from the current flow of the equivalent circuit, which should be accounted despite geometry dependence of the output. This is because this condition exists at the switch at a single point. These are determined as follows for Equation 3.33 through Equation 3.37:

$$i_N = i_{leak} - i_0 - i_R - i_L - i_C \quad (3.33)$$

$$i_0 = \frac{1}{2N^2} \frac{du_s}{dt} \quad (3.34)$$

$$i_R = \frac{l}{2N^2 c C_0 R_L} u_s \quad (3.35)$$

$$\frac{N^2 L_L}{L_N} \frac{di_L}{dt} = \frac{\omega_0^2}{2} u_s \quad (3.36)$$

$$i_C = \frac{C_L}{2N^2 C_0} \frac{du_s}{dt}. \quad (3.37)$$

The boundary conditions at the output are usually to consider the output open ended, in which case the currents at the output are all equal to zero for Equation 3.38:

$$i_a = i_p = 0. \quad (3.38)$$

Yan *et al* also diverge from the work of Pal'chikov in that they explore loading effects more thoroughly and the effects of resistive losses. Comparisons of the results of this model and the first two frequency model can be found in the chapter on results. This

model is rather complex compared to other models and can be solved using a Godunov scheme or finite element method. Yan and Parker state that this model generally is most applicable to spiral generators with a large number of turns, thin copper tape, and large mean diameter.

3.1.6 Design Considerations

There are several configurations of the spiral generator to be considered during design. The first and most simple of these considerations is the placement of the switch. The switch may be placed either between the inner two ends of the active and passive conductors or on the outer two ends with the output tap being on the opposite. This will not significantly impact the waveform further than changing the polarity of the output waveform.

Other than the geometrical parameters discussed earlier such as width, winding diameter, or number of turns, the spiral generator can also be wound in different ways. The first of which shown in the initial presentation of the spiral generator by Fitch can be found below in Figure 3.6.

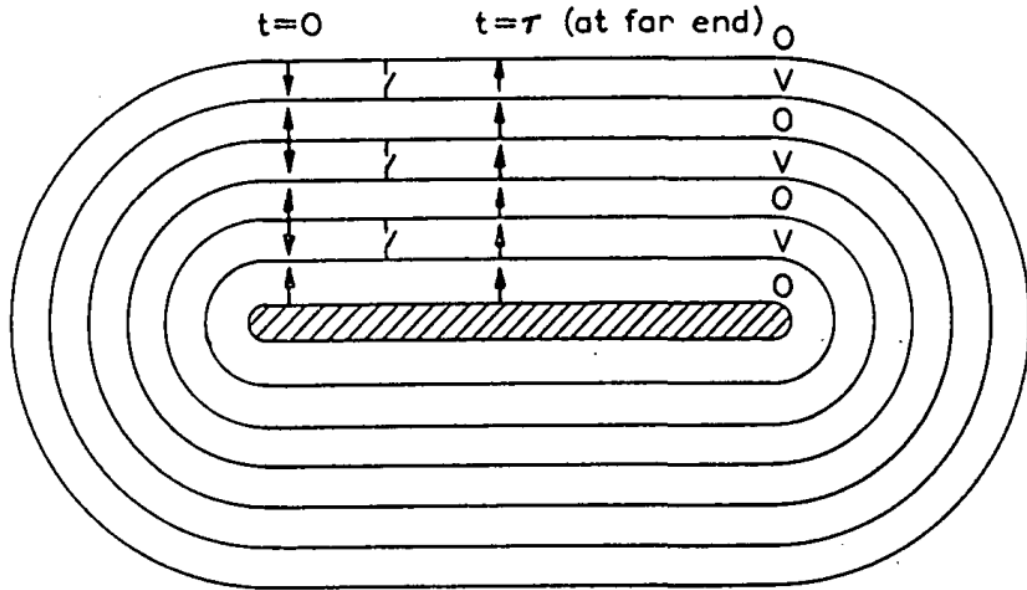


Figure 3.6 Stacked Stripline Generator Configuration [4].

In fact, the above configuration is an alternate form of the spiral generator for which there is little difference between the two. This configuration has seen little exploration but has the potential for some advantages over the spiral generator. The first is that of the ability to operate with a lower winding cross-section without the sacrifice of low input capacitance – though a possible disadvantage could be that the lower cross-section does not allow space for a ferrite core. This lack of space also creates difficulty for placing a switch on the innermost winding.

Another configuration of interest is that of the twin spiral generator with a parallel connection. This configuration is put forward by Fitch in his initial presentation [4]. Similar to the first configuration, there has been little if any research utilizing this configuration published. This is a bit harder to model with there being no clear way to create a summation of the behavior of both generators. Some advantages of this configuration maybe allow the ability to create a generator with more available energy without increasing the length or operating capacitance of each generator. Thus – a generator in this configuration could be

devised out of two generators which the same frequencies. A primary advantage of this configuration is the presence of only one switch. A depiction of this generator can be seen below in Figure 3.7.

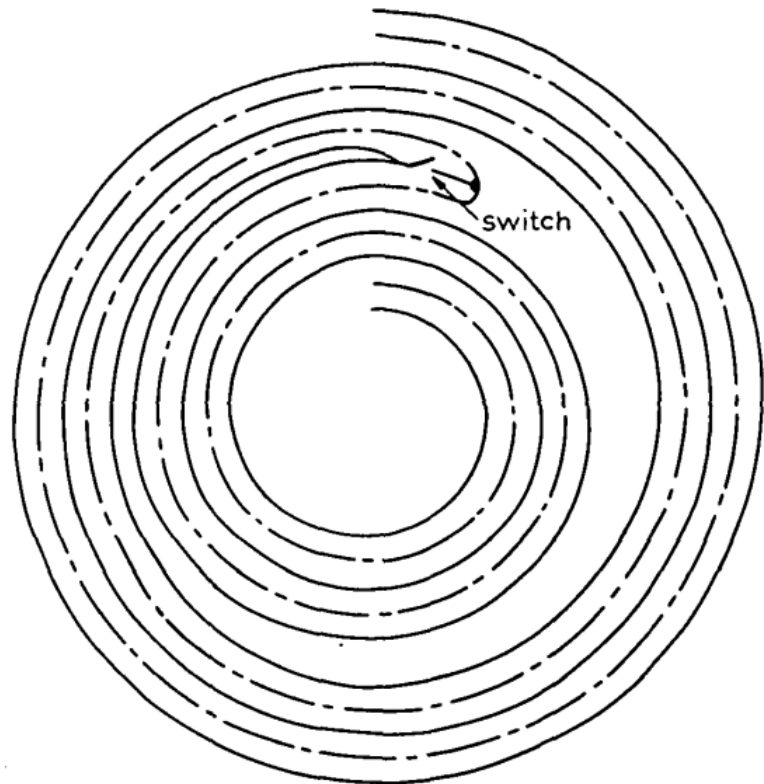


Figure 3.7 Twin Generator Configuration [4].

Other than physical configurations, another design consideration is that of materials used. These materials take the form the material used for the insulation, conductors, or a ferrite core if one is included. The insulator must be considered for the cases of the capacitances, losses to dielectric, and dielectric breakdown strength. The conductor should be considered for the skin depth, wave propagation speed, and inductance. The most important properties for the material for the insulation and conductors are that of the permittivity and permeability respectively. As seen from the previous equations on the frequencies, propagation speed, inductances, and capacitances, these two properties are

seen often. A list of the properties of common conductors, insulators, and can be found below in Table 3.1. This is followed by some notes on materials usage in past studies.

Table 3.1 Electrical Characteristics of Generators Explored.

Conductors			
Material	Resistivity (Ωm)	Conductivity (S/m)	Relative Permeability
Copper	1.68×10^{-8}	5.96×10^7	1.0
Titanium	4.20×10^{-7}	2.38×10^6	1.0
Aluminum	2.82×10^{-8}	3.50×10^7	1.0
Silver	1.59×10^{-8}	6.30×10^7	1.0
Insulators			
Material	Relative Permittivity	Dielectric Strength (MV/m)	Resistivity (Ωm)
Kapton	2.78-3.48	30.3	1.00×10^{12}
Mylar	3.10	27.6	1.00×10^{18}
PVC	3.18	30	1.30×10^{16}
Teflon	2.10	60-173	$1,00 \times 10^{23}$
Mica	2.5-7	39.4	$1,00 \times 10^{13}$
Transformer Oil	2.10-2.40	10	3.50×10^{13}

For the generators used in this study, Kapton and Copper were used as the materials to construct the generators. However Yan and Parker used Mylar as their insulator and the PT-55 seemed to use a PVC or Mica sheet material. Other generators use oil submersion to prevent arcing across the edges of the conductors.

Switch selection plays an important role in design of a spiral generator as discussed before but while we made the switch inductance negligible by overbuilding our generators other methods may include that of using specialized switching such as that explored by Yan and Parker and that used on Spiral Generators found in the decade module such as the one seen below in Figure 3.8 and **Figure 3.9**. This generator is known as the PT-55.



Figure 3.8 The PT-55 professionally manufactured Spiral Generator.



Figure 3.9 Front face of the PT-55.

This generator above is a good example of how to design very high voltage generators with a decent efficiency when overbuilding the switch is possible rather than the generator. It has a low number of turns and very low conductor width the second of which would result in a low switching efficiency if not for the specialized radio-isotope switch. This switch of course is solid state which is a valuable and cost-saving method in spiral generator design. While the exact rating of this generator is unknown the insulation appears to be a mica-based insulator sheet which is thick enough to allow a very high charging voltage in order to offset the low number of turns. Based on the design of the

decade half-power module this generator and the others were likely designed in such a way to allow precise timing in triggering the large 500 kJ module.

3.2 Materials Used

Generators built for the proof of concept use simple material. For the generators in this effort the conductors consisted of copper foil tape of various widths, with the paper backing left on for ease of winding. This foil was used to retain similarity to past efforts, and because of the ease of obtaining and ease of applying solder to the material. The insulating material was Kapton tape due to its high dielectric strength and low thickness, so to maximize the output capacitance of the generators.

Selecting a switch is important for manner smaller generator designs, however exploration of the effects of switch characteristics was not a desired path. For this purpose, the generators used had a high inductance and long conductor length as to allow the use of simpler switches capable of higher currents as these generators were less sensitive to switch characteristics. This allowed the testing of generators mostly independent of switch efficiency factor ε_1 . Due to the high voltage involved a simple 15kV clacking relay was used as the switch for each generator. Higher voltage testing would result in a lower corona efficiency factor ε_5 due to the long lengths per turn. For the low voltage tests, the switching was performed using a simple flick switch. For generators requiring more of the switch such as higher life-span, precise control, higher currents, or automation, solid-state switches can be used to with lifespans in the millions of cycles [14], [34]. For generators requiring very high charging voltages, high current discharges and extreme switching characteristics it is more useful to use a spark gap switch, or dielectric puncture switch and compact versions [23].

For sensing the output voltage, many oscilloscopes are not fast enough to read the waveform output by a spiral generator which have a peak-to-peak time in the tens of nanoseconds. To meet this requirement a Tektronix TDS 754D oscilloscope was used and can be seen below in Figure 3.10. Capturing the output of the generators at high voltage also poses a problem in that a charge can build on the outside surface of a high voltage attenuator and release a portion of this charge into the measurement line when the path to be measured is shorted to ground. This is in addition to the fact that attenuators which filter the output often cannot read the output of a spiral generator for the same reason which drove the oscilloscope selection. No low pass filters can be used to protect equipment for the same reason. Additional problems arise for high voltage sensing due to the available attenuators having a relatively low pulsed peak-to-peak voltage rating of at most 80 kV.



Figure 3.10 Tektronix TDS 754D Oscilloscope.

The TDS 754D is an old oscilloscope but well suited for work with spiral generators and other devices which output waveforms over a few hundred nanoseconds. This is due to its high 2 gigasample per second sampling rate, and its operating frequency of 500 MHz. While the above is true it is not ideal for capturing waveform data in detail as it operates using an old phosphorous screen and there is no easy way to retrieve waveform data directly short of taking a photograph of the screen and digitalizing it as has been done in this effort. This of course is not true if one has old floppy disks and floppy disk readers available.

The winding machine later constructed and used to fabricate many generators for the proof of concept and the parametric analysis is a simple construction. This machine

utilized 3D printed parts for ease of fabrication. It consists of four completely 3D printed wheels and one large wheel made from laser cut plastic and 3D printed parts. The large wheel is for the generator to be wound around while the four smaller wheels are to supply material for the winding. The decision to use 3D printed parts for the wheels was primarily to accommodate different sizes of material rolls for the conductors and insulators. The entire assembly is mounted onto a plastic baseplate and 3D printed gates are used to keep the conductors in alignment during the process. Due to the varying torque required a simple connector for a socket wrench was included on top of the large wheel to drive the system. While not very scientific, this simple solution allows torque to be increased or decreased informed by feel alone. This proved to be a decent enough solution to allow easy fabrication of generators with a relatively large number of turns.

3.3 Approach Taken

This exploration first started with attempts to construct a working spiral generator driven by insight from other explorations into spiral generators and the apparent simplicity of the generators. The first prototype generator appeared to show some multiplication during tests but was unable to be reproduced consistently. This was later found to be due to having a too low resistance of a charging resistor and due to the generator having much too low of a transit time for the slow rise time of the switch and thus a low switch efficiency factor ϵ_1 . The intermittence results produced were attributed to switch bounce in which the output pulse has an artificially sharpened edge due to the shorter effective rise time. Several prototypes failed due to similar problems before a replication of the generator used by Yan *et al* was finally successful at low voltage [7]. This generator was used to provide the initial

results and give insight as to how to approach future work including the parametric analysis.

The equivalent circuit model described in the previous section was used to provide further design considerations, and it was using this model that the effects of switch bounce were confirmed by simulating the switch opening early during operation of the generator. This model also described well the impact of spiral inductance on the efficiency factor. In addition, it was possible to explore some of the effects of different loads on the generator. The equivalent circuit model was later used to compare to different built generators used in initial results, though noting once again that this model is inadequate for simulating the oscillation period of the generator.

The first failed attempts were all fabricated without a winding mechanism to properly create the spiral geometry. This necessitated the use of wider conductor materials to ensure proper alignment which reduced the inductance of the generator and caused many of the initial problems. In addition, winding by hand would leave large gaps and folds between the layers, which would make the circuit diagram and some of the equations less representative of the actual function of the generator.

This machine shown in Figure 3.11 would later be modified to produce generators with a greater inner diameter in order to reduce the resulting generators sensitivity to switching characteristics. Because fabricating spiral generators with had been found to be much more difficult when done by hand, this winding machine was what allowed pursuit of the future work of the parametric analysis. The newly fabricated generators could be produced quickly, be operated all from the same switch, and use the same load during testing.



Figure 3.11 Winding System Used for Fabrication.

The winding system seen in Figure 3.11 does work but not as well as would be hoped. In order to modify the system to produce more consistent windings in a shorter period of time the system would need to be motorized with a tension control system added. This can be done in several ways. Either with braking systems, independent motorization of each feeder mandrel, and or the addition of a mandrel in-between that is mobile for either

computer adjustment or tension force adjustment using a spring. This winding system however simply used a friction-based gating system to both ensure alignment of the foil and to provide tension via friction to the conductor. This gating system can be seen in Figure 3.12 in use for a winding in progress. The system also used the peel force of the adhesive Kapton tape in order to provide tension for the insulator. This unfortunately causes problems due to tension not being constant or controllable as too high of a tension will result in stretching or folding of the materials and too low will allow slack and migration of the material out of alignment.



Figure 3.12 Alignment and Friction Gate used for Winding in Progress.

The above gating system has a proposed replacement for possible future work. This replacement can be seen in below in *Figure 3.13*.

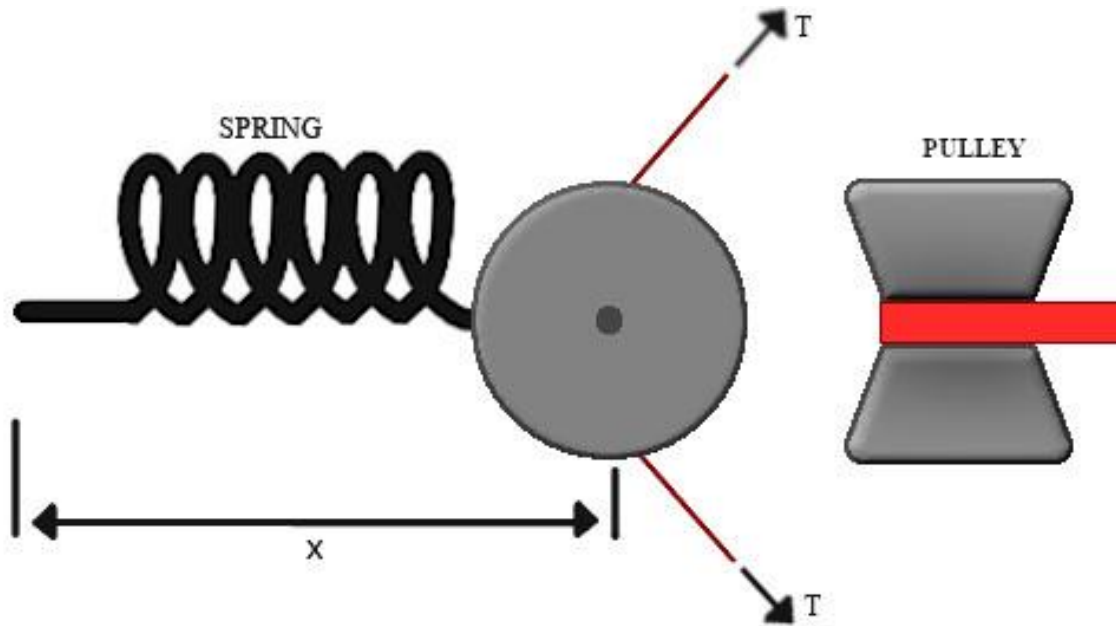


Figure 3.13 Pulley System to Replace Gate System.

The above Pulley system will be used in a future upgrade to the winding system and provides solutions to multiple problems. This system is effectively a pulley allowed to freely move along a linear rail on the x-axis shown above. The pulley will be a midpoint for the winding material as it travels to the primary winding mandrel. This system allows us to remove slack via displacement of the pulley along the X axis rail, as well as determine the tension via displacement through extension of the spring. Tension can be removed by increasing the feed rate of the motor controlling the feeder roll in question, or added by decreasing the feed rate of the roll. This will cause the spring to shorten or lengthen as tension decreases or increases, allowing no additional slack into the system. This means that a method for measuring the displacement of the pulley along the x-axis will allow us to determine the x component of the tension on the material to be wound into the spiral and could allow a controller to be programmed to fully automate the system.

After fabrication of the winding machine, the first generator fabricated with that method was a success. This generator can be found below in Figure 3.14. It was tested using a small flick switch and showed that the machine could be used to make working generators. This generator tested early in this exploration was done using only low voltage, and this is because the charging voltage does not significantly alter the waveform or function of the generator. This is only true so long as the insulating material has a dielectric strength strong enough to withstand that voltage.



Figure 3.14 A 30-turn spiral generator fabricated as a first test.

The 30-turn generator was fabricated with the intention of simply testing the winding system and before a good understanding of the effects of geometric parameters on

generator function was obtained by the author. As such this generator is unsuitable for high-voltage testing but if immersed in oil should still be able to produce a high-voltage pulse without much trouble. Nevertheless, the generator was tested at low-voltage which was an approach surprisingly not yet seen. A close photograph of the layers of this generator upon being removed from the mandrel post-testing can be found below in Figure 3.15.

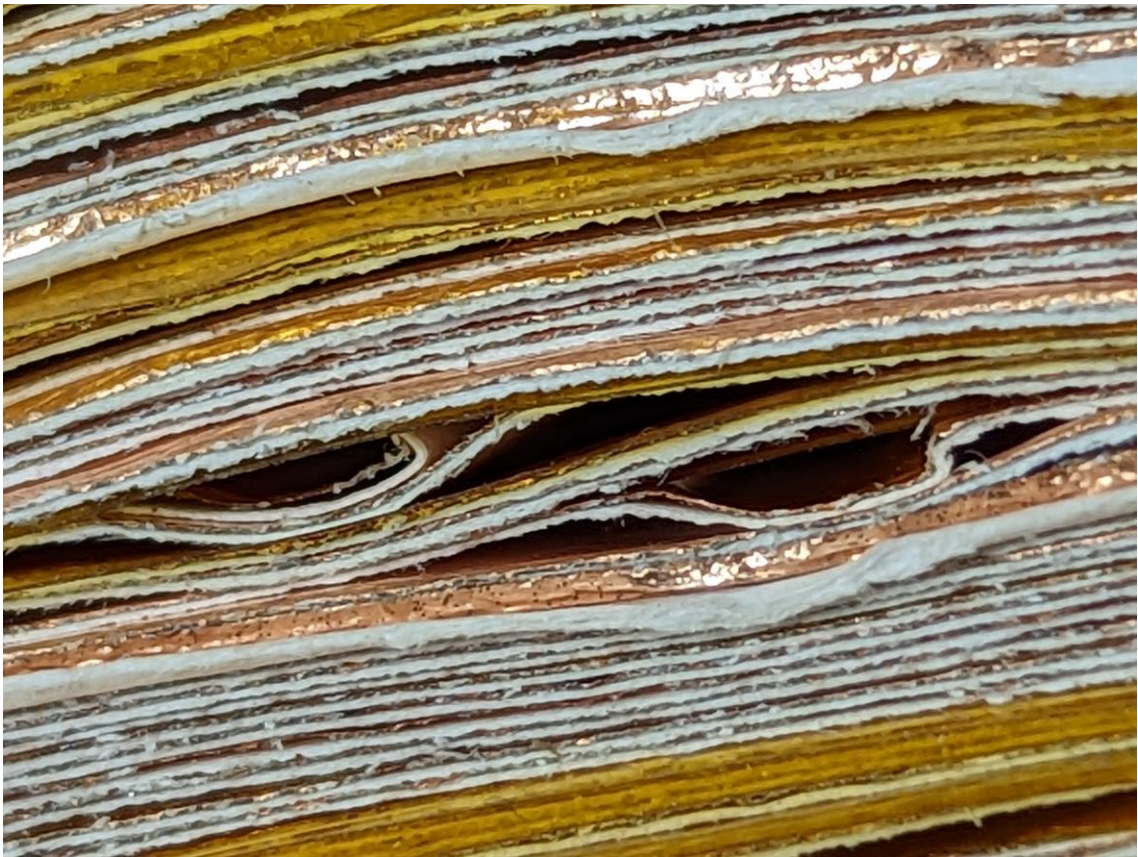


Figure 3.15 A close up view of the layers of the 30-turn spiral generator.

Figure 3.15 shows an obvious flaw in the winding of the 30-turn generator. This did not appear to significantly impact the function of the generator at low voltage but may cause the generator to fail more easily due to arcing in other generators should this occur to the insulator as well as result in a small efficiency loss. This shows the importance of a

proper winding system which does not result in these flaws and folds. There are two other flaws in the generator like this one.

A high-voltage spiral generator was wound next and tested. A close photograph of the layers of this generator can be found in Figure 3.16. Due to concerns of damaging the only oscilloscope capable of accurately capturing waveforms over nanosecond timescales the decision was made to use an adjustable spark gap and estimate the high voltage output. This simple adjustable spark gap can be found in Figure 3.17. This would have the effect of a pulse sharpener on the output and would reduce the possible output voltage by a minor amount. It was found that the 52-turn generator was very inefficient. This inefficiency was attributed to the very low output capacitance being on the same order of magnitude as the capacitance of the probe and adjustable spark gap used but was too drastic to be explained by the reduction in output voltage of the gap alone. This would effectively make the efficiency factor ε_4 very low due to the lack of available energy in the charged passive conductor with the high length causing an increase in resistive losses.



Figure 3.16 A close up view of the 52-turn spiral generator.

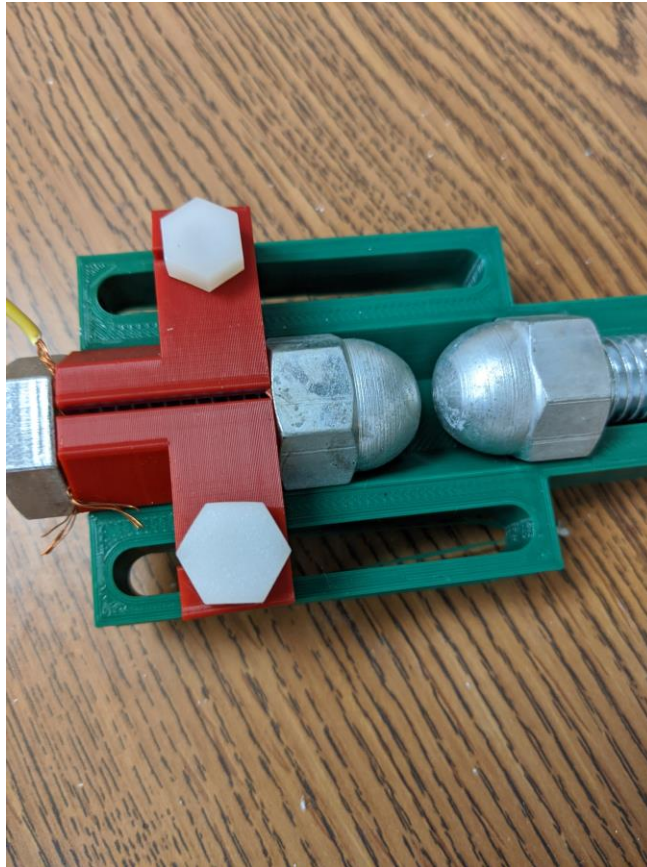


Figure 3.17 A Simple Adjustable Spark Gap used in Testing of the 52-Turn Spiral Generator.

The 52-turn spiral generator seen in Figure 3.16 was wound on a mandrel of the same configuration. This generator was originally wound in this manner with a very low width in part due to misunderstanding of the origin of the efficiency of the generator and an incorrect assumption that the switch and generator inductive ratios were dominant in the efficiency. Both generators wound in this study are done with Kapton and copper foil and this was useful in that as winding progressed the layers could be observed through the transparent insulator. This allowed the operators of the winding system to compensate as needed if the layers started to become misaligned. The use of this Kapton as an insulator was because it was transparent but rather that the winding system required tension to work correctly. This tension was provided using the peel force of the Kapton tape and worked

well for generators up to 30 turns. Higher numbers of turns resulted in the Kapton tape stretching and folding in upon itself which could be addressed using a gate to ensure alignment just before reaching the mandrel as was done with the copper foil on the 52-turn generator.

As is evident by the fabrication process described above there are many ways to wind a generator but it is imperative that the generator be wound with as little defects as possible. To do this by hand is improbable and the best way to wind these generators is by a machine similar to our own. This was found through trial and error and a collection of generators were fabricated while others were simply found. A photograph of part of this collection can be found below in Figure 3.18.



Figure 3.18 A Collection of Spiral Generators.

The generators seen in Figure 3.13 include the ones fabricated and tested in this thesis but also a few that have not been discussed. That includes the small generator which failed due to a low winding diameter resulting in very low efficiency as well as the black generator which failed due to a low number of turns and too much distance between the conductor layers. The other three which look quite similar were manufactured for the Decade Half Power Prototype.

Chapter 4. Results

Two of the four generators fabricated for this study showed consistent and significant multiplication. The four generators fabricated were a 14-turn generator constructed of thick copper sheet wrapped in overlapping electrical and PVC tape, a 30-turn generator constructed from wax paper insulation and 2” wide aluminum tape, and two generators fabricated with Kapton tape and copper foil tape of widths 1” and 1/5” with 30 and 52 turns respectively. The last two are the generators of interest and offer a proof of concept and insight on how to proceed with future research. The results for the 30-turn generator can be seen below in Figure 4.1, with the electrical characteristics and geometric parameters of both generators present in Table 4.1. Table 4.1 also contains the electrical and geometric characteristics reported for each of the generators used in Yan’s geometric analysis [7]. This is the case as we use the generators from the geometric analysis for comparison to the results of the simple two frequency model.

Table 4.1 Electrical Characteristics of Generators Explored.

Turns (#)	L_{out} (μ H)	C_{in} (nF)	Mean Diameter (mm)	Combined Layer Thickness (mm)	Width (mm)
30	183	52.2	146.3	1.8	25.5
52	660	25	153.7	1.8	5.1
12	34	10.5	120.0	0.3	12
24	111.8	22.8	120.0	0.3	12
36	240.2	36.3	120.0	0.3	12
48	414.3	51.4	120.0	0.3	12
24	126.2	9.1	120.0	0.3	5
24	93.8	43.5	120.0	0.3	25
24	70.8	85.9	120.0	0.3	50
24	18.4	6.9	40.0	0.3	12
24	57.2	14.3	80.0	0.3	12
24	159	29.4	160.0	0.3	12

It should be noted that despite being made out of the same material, and the only geometric

parameter difference being number of turns, that the first two generators are thus very different in terms of input capacitance, turn inductance, and output capacitance.

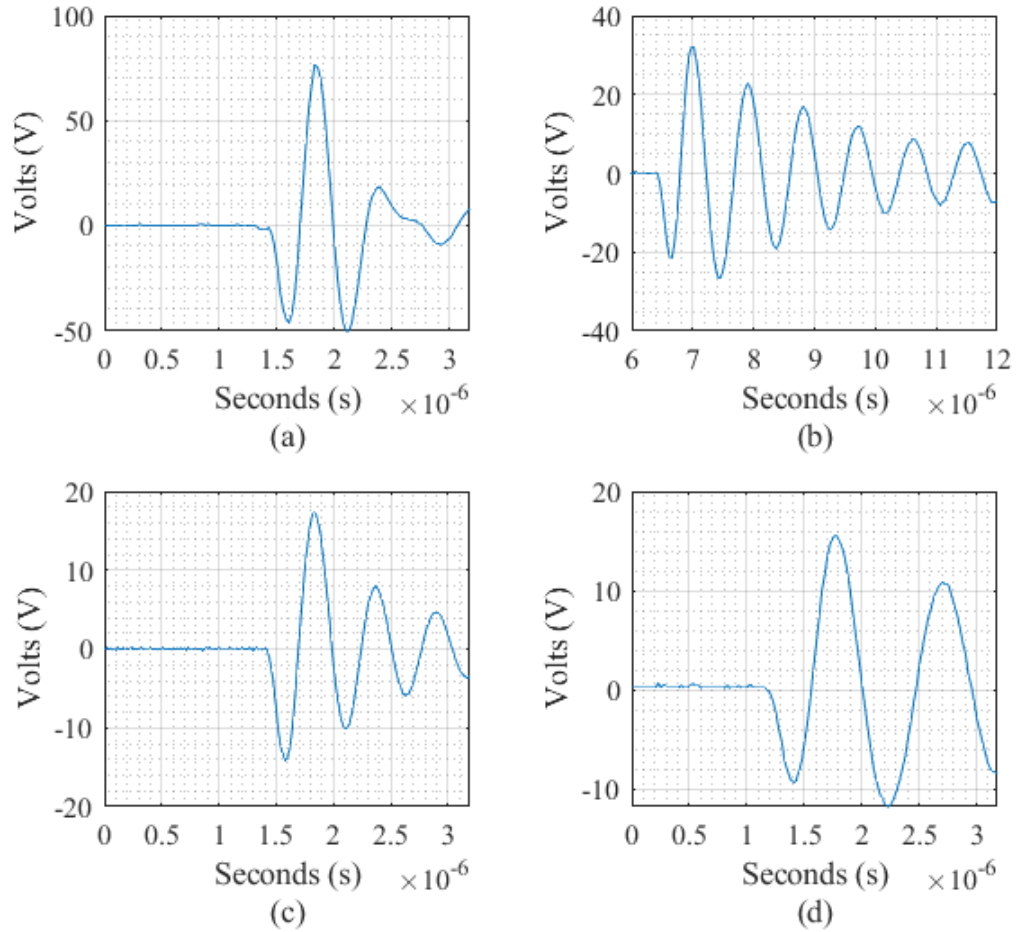


Figure 4.1 Results for 30 Turn Spiral at a) 2 V with no Switch Bounce, b) 4.1 V with Switch Bounce, c) 2 V with Switch Bounce, and d) 4.1 V with Switch Bounce.

Over the course of testing switch bounce resulting from the simple flick switch used for low voltage testing was a common occurrence. Occurring at any point within the first few hundred nanoseconds of the output waveform, bouncing of the switch contacts results in oscillation at a singular frequency. This is thought to be LC oscillation inside the generator, but the frequency is inconsistent. This can be seen by comparing Figure 4.1 a)

b) where the waveform oscillates at two different singular frequencies. Further low voltage testing at increasing voltages can be seen below in Figure 4.2.

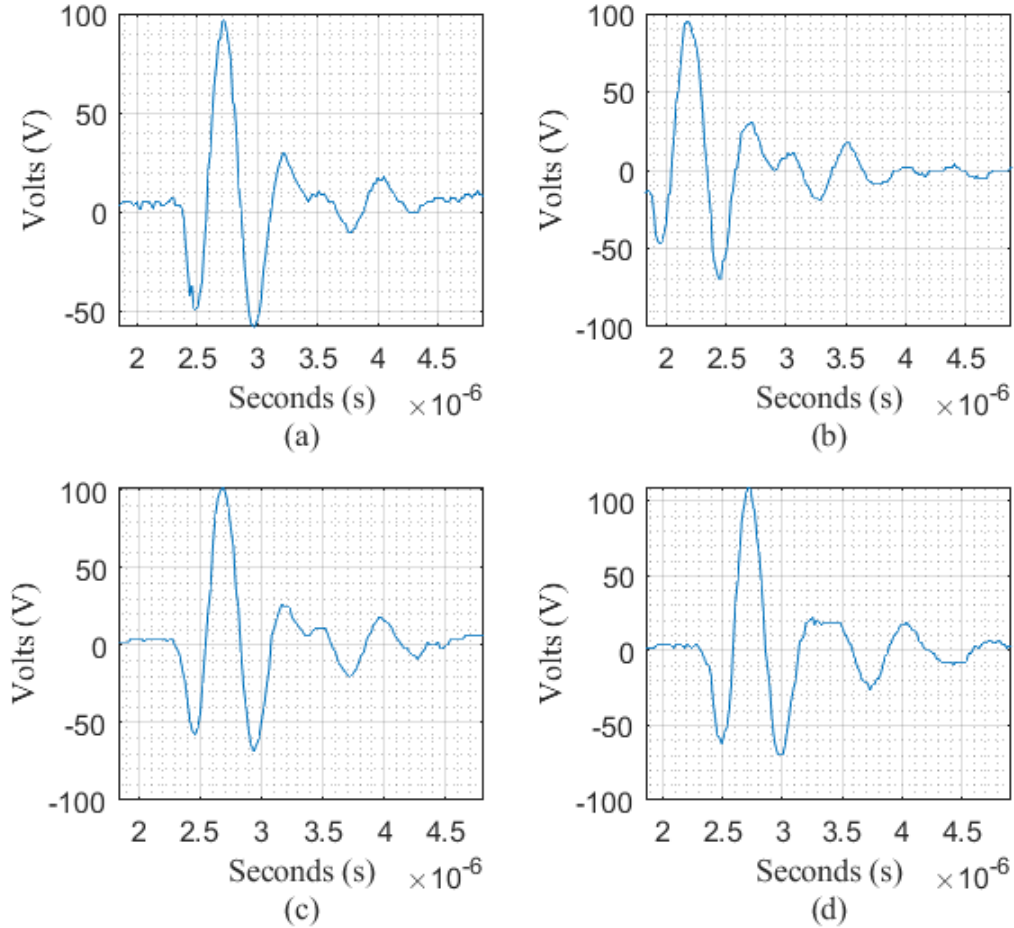


Figure 4.2 Experimental Results for a 30 Turn Generator, All Cases were Performed at a Charging Voltage of 4.1 V.

The results presented in Figure 4.2 do not contain switch bounce cases, which were notably less common as voltage increased. Multiplication factor ranged from 24.5 to 28.5 for these tests showing an efficiency for the 30 turn spiral generator as $\epsilon_{ff} = 41\%$ to $\epsilon_{ff} = 46\%$. The increase in efficiency is thought to be partially artificial from the change in oscilloscope as the oscilloscope used in the previous test cases was too slow and resulted in trimming. The other component for the increase in efficiency can be attributed to

shortening of the leads connecting the switch to the generator thus reducing effective switch inductance. The final series of tests at increasing voltages can be found in Figure 4.3 and Figure 4.4.

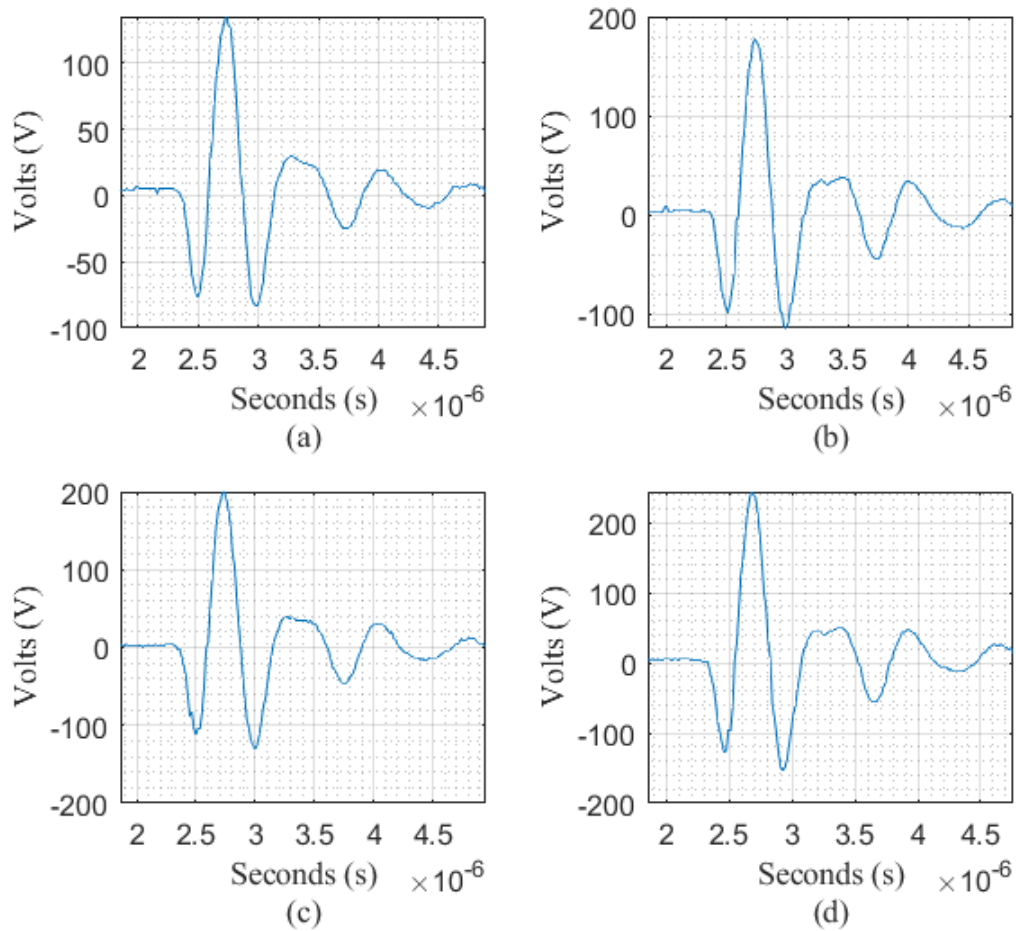


Figure 4.3 Results for 30 Turn Spiral Generator at a) 5 V, b) 6 V, c) 7 V, d) 8 V on a Tektronix TDS 754D Oscilloscope.

The results presented in Figure 4.3 show output voltage waveforms for several increasing charging voltages. With the lack of results for spiral generators operating at low voltages in other studies, an interesting phenomenon of increasing efficacy with charging voltage is observed. Note that for case a) a multiplication factor of 28 and efficiency of nearly 47% is achieved. These both increase with charging voltage with case b) showing a

multiplication factor of 30 and efficiency of over 50%, case c) showing multiplication factor of 28.6 and efficiency nearly 48%, and case d) showing a multiplication factor of 30.5 and efficiency of 51%.

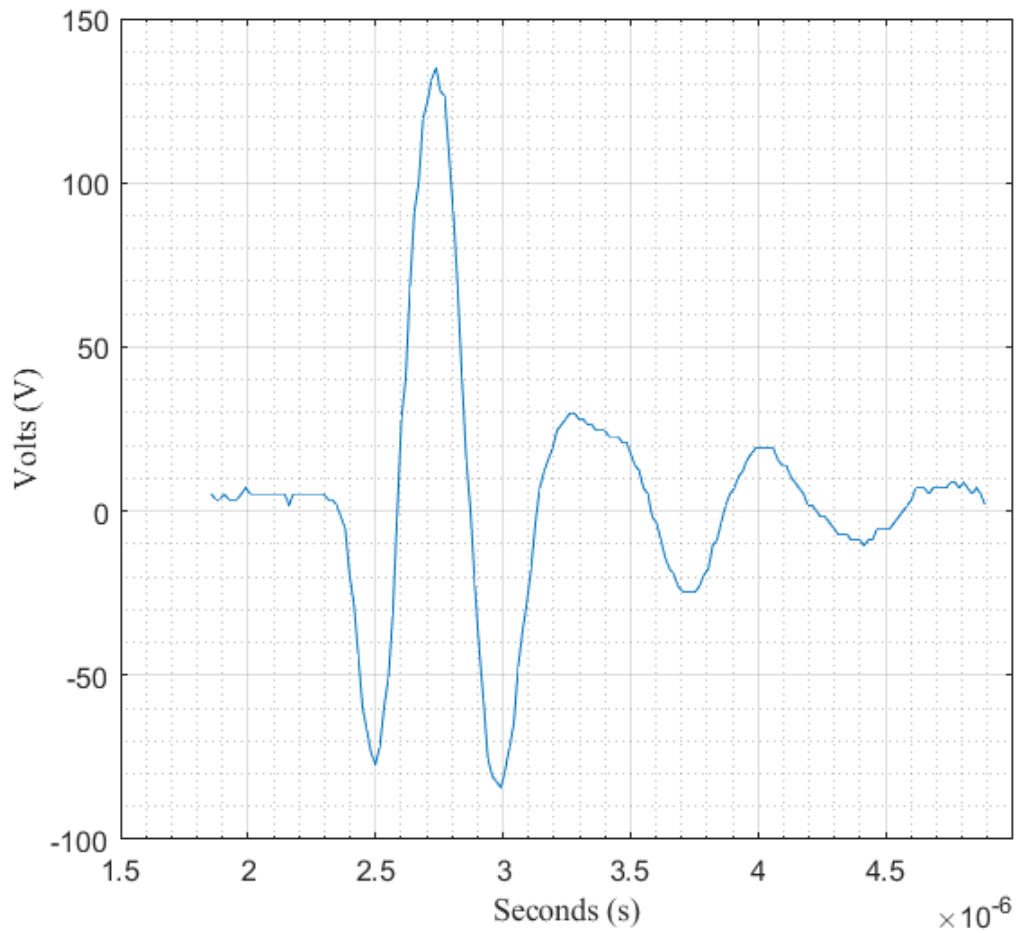


Figure 4.4 Final Test Case for a 30 Turn Generator Charged to 9V.

For the final test case shown in Figure 4.4, the 30-turn generator was charged to 9 V. This resulted in an output with a peak voltage of 280 V, showing a multiplication factor of over 31 and efficiency of approximately 52%. It is notable with all test cases involving the 30-turn generator that except for cases involving switch bounce it is shown that the waveforms are composed of identical frequencies. This is again due to these frequencies

being determined by geometry and electrical characteristics solely and as such one configuration including load and operating switch will ideally produce nearly identical waveforms with the only difference being the amplitude.

Some initial high-voltage testing was also performed, but due to fear of damaging the only oscilloscope fast enough to clearly capture the fast waveforms produced the voltage was approximated using an adjustable spark-gap as a load. This second set of tests was performed on the 52-turn generator which was better insulated for this task and over the duration of the experiment the generator was charged and fired at levels between 1 kV and 5 kV. Firing the generator using a high voltage clacking relay, the results approximated based on spark gap distance is summarized below in Table 4.2.

Table 4.2 Summarized high-voltage results of a 52-turn generator.

Charging Voltage	Average ϵ_{ff}	Multiplication Factor	Best Output
1 kV	0%	0	N/A
2 kV	6 %	6	12 kV
3 kV	6 %	6	18 kV
4 kV	7 %	7	28 kV
5 kV	N/A	N/A	Generator Failed

The results from Table 4.2 are approximate and summarized over dozens of shots. The generator would fail to cause breakdown across the spark gap used at voltages lower than 1 kV. Occasionally the generator would fail to produce significant multiplication even at voltages higher than 1 kV. This was attributed to switch bounce of the relay reducing the generator efficiency even further as this phenomenon became significantly less common as charging voltage increased due to arcs being drawn across the high-voltage relay as the relay contacts bounced off one another. Most notable from these results is the incredibly low average multiplication efficiency. This is thought to be due to the very low

output capacitance of this generator, with the self-capacitance and capacitance of the spark gap effectively holding down the output voltage.

To have a greater set of data for comparison with the simple two frequency model experimental results with the proper geometric and measured characteristics stated were sought out. This led to the comparison of the model with the experimental and simulated results produced by Yan *et al* during their study of geometric scaling of the spiral generator [7]. The first of these comparisons can be seen for scaling of number of turns in **Figure 4.5** below. These results use electrical characteristics calculated directly from geometry.

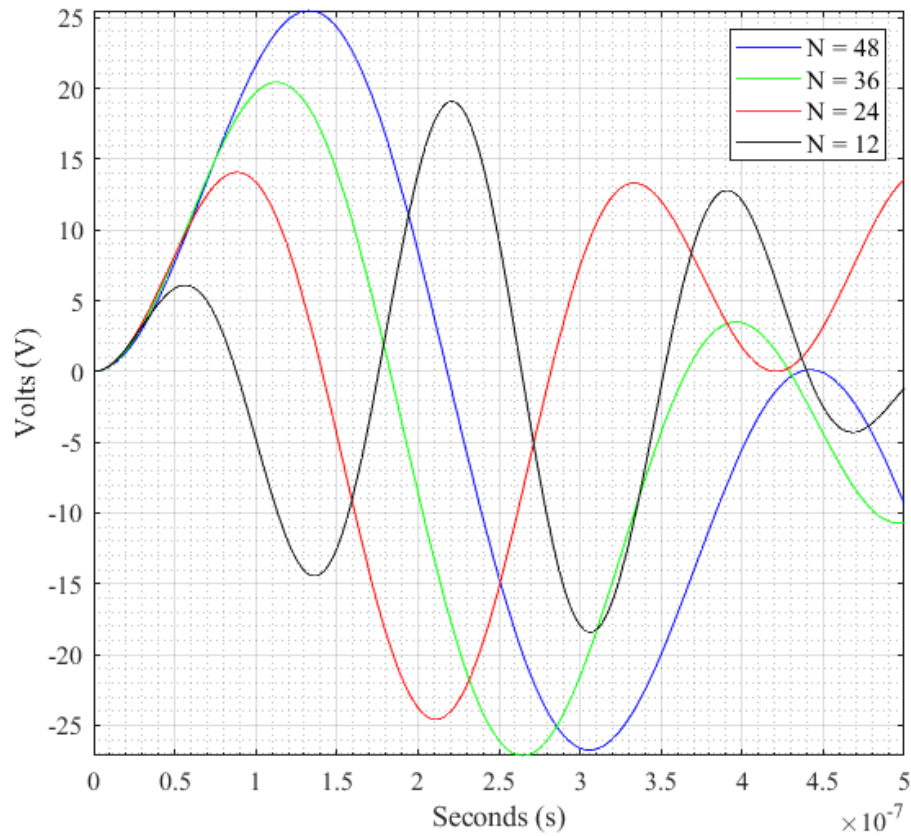


Figure 4.5 Comparison of Geometric Scaling of Turns [7].

The model seems to agree well with the experimental results produced by Yan *et al.* There is a clear agreement with the timescales and damping, with around 15% error in most cases caused by a disagreement with the resonant frequency. This appears to originate from error arising from an incorrect output capacitance. The next comparison set is that of a geometric scaling study focusing on width found in **Figure 4.6**.

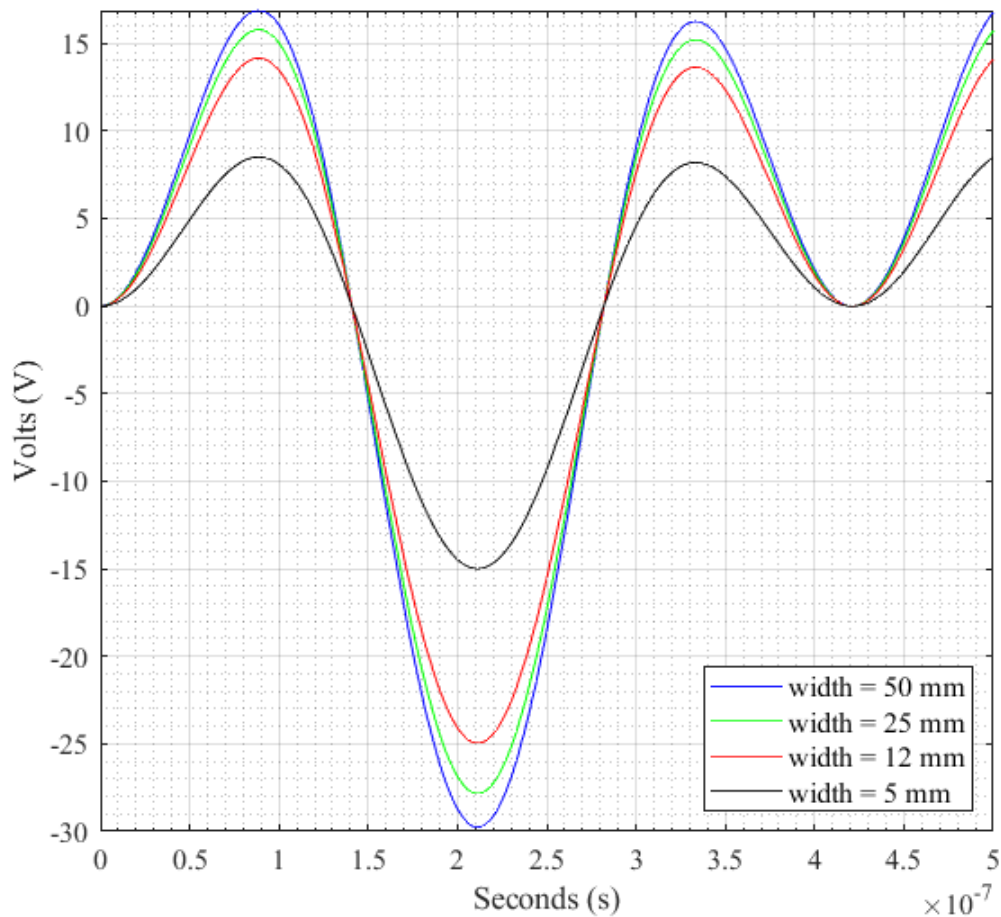


Figure 4.6 Comparison of Geometric Scaling of Width [7].

This comparison shows excellent agreement as well, with the calculated values portraying some interesting trends to be discussed in conclusion. Notably, both frequencies calculated are an exact match with damping consistent with experimental results. The

timescales of the results with calculated electrical characteristics are within 20% and agree well for all widths. This error is once again attributed to errors in output capacitance calculations. The next set in which the mean winding diameter is the geometric property of interest can be found below in **Figure 4.7**.

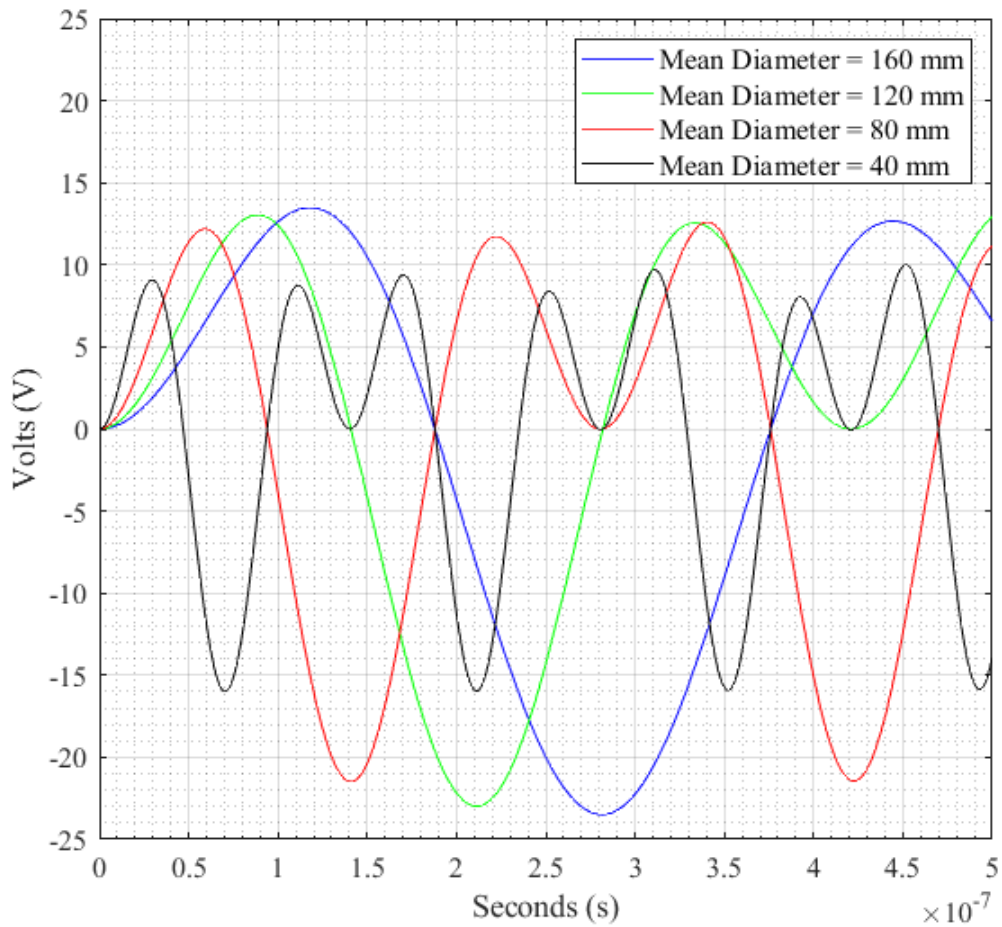


Figure 4.7 Comparison of Geometric Scaling of Mean Diameter[7].

The final comparison shows good agreement in most cases with some divergence apparent in the lowest diameter generator. The timescales are still mostly correct, showing the impact even a small change in resonant frequency can have on the shape of the output

waveform. Again, output capacitance calculations are thought to be the cause of this divergence and errors in timescales. For completeness the next set of results in the following three figures are derived from using the electrical characteristics and conductor length directly reported by Yan et al [7]. The first of these starting in the same order as that of the previous set can be found below in Figure 4.8. It is important to note that there is no damping present for this set.

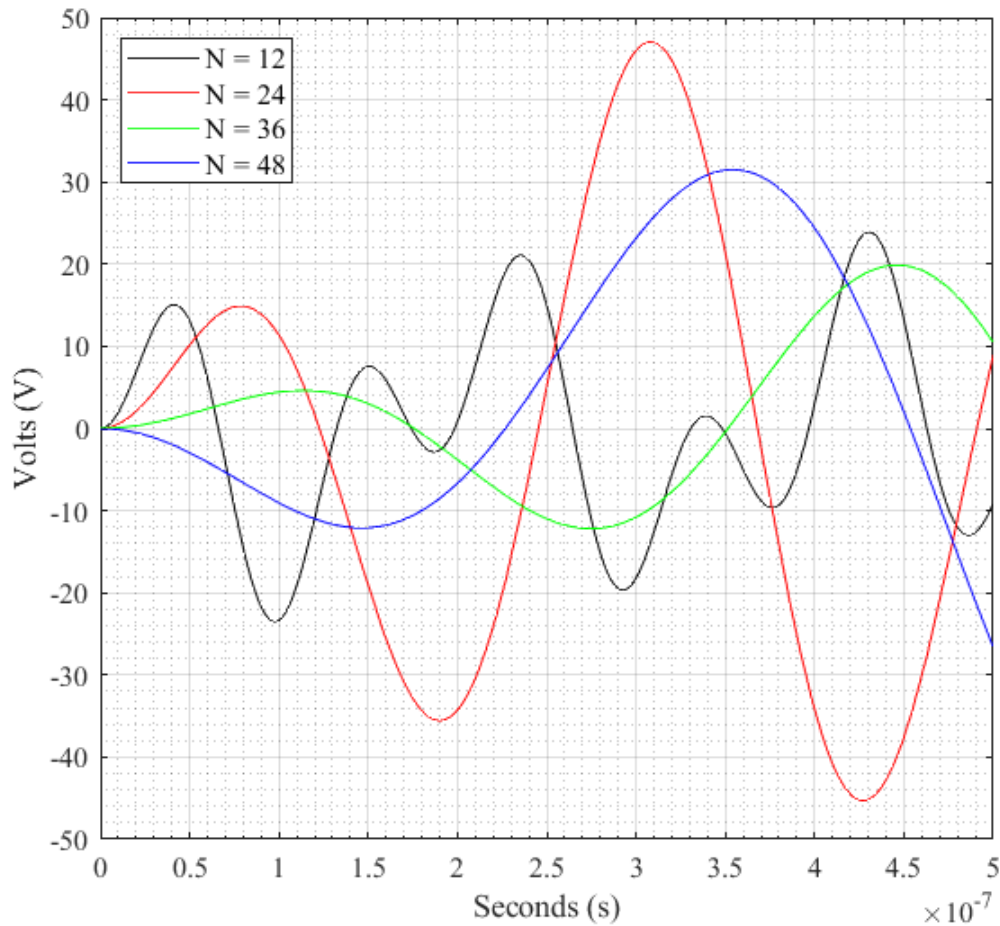


Figure 4.8 Comparison of Geometric Scaling of Turns from Given Values [7].

It is immediately apparent that using the given values for the length and electrical characteristics results in drastically different waveforms for most cases, however the

dominant timescale is still present with the peaks being approximately where they should be. This is an indicator of the dominant frequency being correct while the other is not. The previous set of results made it apparent that the dominant frequency was the transit frequency, meaning that the error resides in the resonant frequency. The next set shown in **Figure 4.9** has this resonant frequency error shown with more clarity.

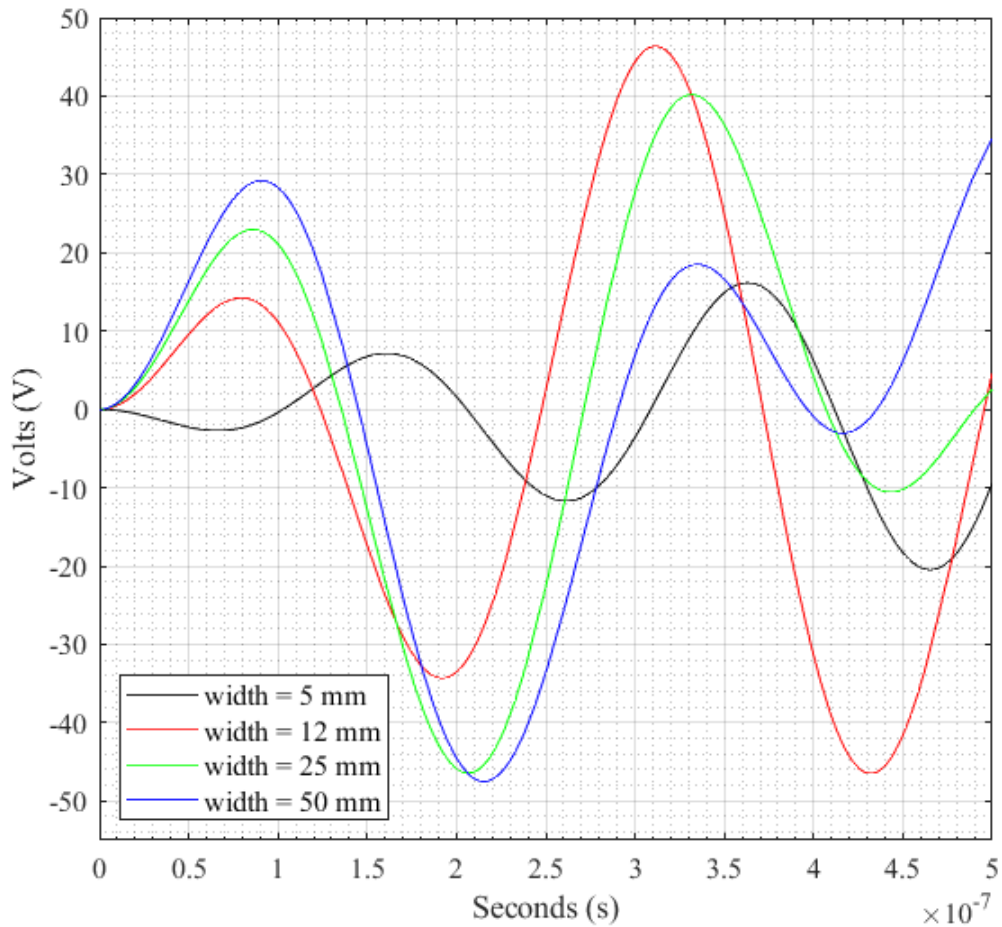


Figure 4.9 Comparison of Geometric Scaling of Width from Given Values [7].

This is a good data set to see the differences in waveform resulting from the resonant frequency error. This is because the transit frequency is approximately the same for each generator for which the waveform was calculated for. It becomes obvious that as the width

narrows and thus the resonant frequency error intensifies, the simulated waveform becomes less representative of the experimental results. This is interesting considering that for this set the resonant frequency from calculated values was the same regardless of width. Next is the comparison of scaling diameter seen in Figure 4.10.

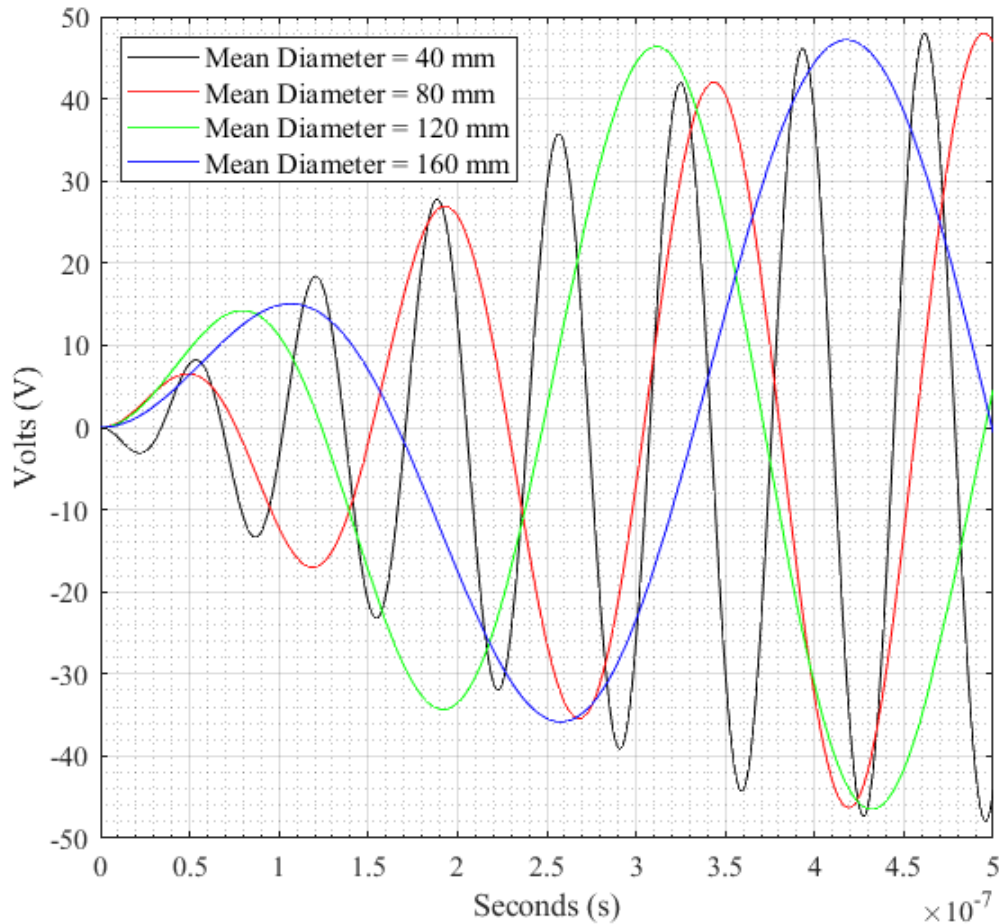


Figure 4.10 Comparison of Geometric Scaling of Diameter from Given Values [7].

While there is little to say about this figure, what can be determined is that it also suggests like the previous that errors in the waveform can be attributed mostly to the resonant frequency as the most accurate waveform is that of the highest length and the least

accurate is that of the lowest length or that of the most dominant transit frequency to that of the least influential transit frequency.

Chapter 5. Conclusion

The problem this work originally set out to solve was the lack of a simple and straightforward written process for fabricating spiral generators and simple models to inform the design of those generators. A spiral generator is a pulse compressor which is charged to a voltage and when the operating switch is closed produces a voltage pulse with precise timing at a voltage which is the charging voltage multiplied by the twice the sum of its layers.

5.1 Conclusions Pertaining to the Hypothesis and Objectives

This research began with the hypothesis that spiral generators can be manufactured within a simple lab environment to generate HV pulses with extremely precise timing and low jitter. To approach this hypothesis a set of objectives were selected. To approach first to illustrate the functions and applications of spiral generators it was determined that a few generators would be fabricated for experimentation. The second to explain the relevant equations, physics, and theory relevant to the spiral generator would be approached by explaining different configurations, why they work and how they work in addition to the working equations and physics, in addition to the strengths and weakness stemming from these physics. The third objective to show and elaborate on relevant analytical models was to be approached by thoroughly researching the existing models and later included developing the simple two frequency model such that discussion could be taken from that viewpoint. For the fourth objective the parameters of the generator and how they impacted the generator's function would be explored. This was to be done with insights on previous generators and ones fabricated as part of the first objective. The final objective was to share knowledge on how spiral generators were fabricated and how they could be fabricated.

This was to be done by showing different configurations, researching methods used by other researchers, and fabricating our own. This objective was notably added well into research due to problems with fabrication by hand.

5.2 Conclusions of Approach and Methodology

Now that the intended approach is known, the actual approach as it manifested will be discussed. This work focused heavily on simple methodology for determining the behavior of the spiral generator in both modelling but also focused on low voltage testing. The latter held promise for uncovering relationships that could be used to determine the efficiency factors of the generator. A winding system for generators and initial proof of concept design was desired. The process of addressing the objectives began with a literature survey on previous research done on spiral generators. This gave insight on all objectives but was most useful for addressing the second objective of elaborating on the driving physics and fundamental equations pertaining to the spiral generator.

This was to make the fabrication more streamlined and more trivial than fabrication by hand. The winding system was fabricated and worked for simple designs, however there are improvements to be made. Using this winding machine, generator designs can be chosen to allow easy variation of parameters with the design having a strong operational independence from the switch. This also allowed the use of a singular and very simple high-voltage relay for all high voltage testing, and a simple flip switch for all low voltage testing. Two generators were fabricated for testing. A 30-turn generator was fabricated for testing at low voltages with a simple flick switch, whilst the 52-turn generator was intended for high-voltage testing using a high-voltage relay and an adjustable spark-gap load.

Early in the testing process when a high voltage insulation was needed, the decision was made to use Mylar as the winding insulator. This turned out to be a poor decision as mylar insulators showed a tendency to rip and tear very easily at the thickness desired for testing. This along with the lack of a system to consistently cut the mylar without damage led to a different insulation being chosen. Kapton tape insulation was chosen later due to coming in rolls of proper size and having a higher dielectrics strength. This had its own problems but could be worked around. This tape's adhesive backing caused an additional peel tension when unrolled and the tape would stretch or curl when wound. This would reduce the width of the insulator layer as each new turn was added to a generator during fabrication. This of course actually did help the winding system function as tension from a braking system could instead come from the peel force of the tape. At this point the objective of illustrating the generators' function was complete and insight was gained for use in showing and explaining fabrication methods for spiral generators for the final objective. The fabrication and experimentation of these generators gives additional insight for explaining the impact of geometric parameters for the fourth objective.

As research progressed the lack of clear and easy modelling that could determine the waveform and efficacy of the spiral generator led to the development of the simple model used in this study. The model was developed with the intention of replacing more complex models with one trivial to use using insight gained from the knowledge of the two frequencies of operation of the spiral generator. One frequency is the transit frequency determined by wave propagation and the other is the resonant frequency of RLC oscillation of the generator itself as current flows through the switch, active conductor, and the load. This model for its simplicity depicts the behavior of an unloaded generator quite well, with

a few shortcomings to be addressed in future research. This produced a viewpoint and experience that modeling the generators behavior could be discussed from for the third objective. In addition, this model's use to compare against the results produced by Yan and Parker in their geometric analysis allowed more insight into the physical parameters and how they impact the function of the spiral generator for the fourth objective. The model is connected to reality by the geometric dimensions and material properties of the conductor and insulator layers. For the transit frequency this is the speed of the propagation of the wave via Equation 3.2 down the length of the active line to yield the period in Equation 3.3. This is then used in Equation 3.13 directly for the transit frequency. The resonant frequency is a little more difficult as all LC values of the switch, load, and generator must be accounted for. The values of the switch and load are known in advance. The input and output capacitance of the generator can be calculated via Equation 3.9 and Equation 3.10 respectively, while the inductance is calculated using Equation 3.6 and tables from Grover [8]. This then allows the resonant frequency to be calculated using Equation 3.12. This is enough to get the time-dependent shape of the waveform alone and RLC damping factors may be added if needed.

5.3 Common Problems Faced

It became clear in initial research that the switch inductance was very important early on. Efforts were made with simpler switches and yielded mixed results. This was initially thought to be the fault of switch inductance but was only partially correct. An attempt was made to use transistors for the switching. Transistors available unfortunately were not rated for the current required for larger spiral generators. These transistors could also pose problems for smaller spiral generators as their semi-conductor nature resulted in

fixed rise times that could prevent the generator from operating effectively. These obstacles are what led to the methods used to avoid switch characteristics having a major impact on generator performance. These methods allowed focus to be more so on the design and function of the generators themselves as switching characteristics effects are more commonly explored.

Switch bounce was also an issue especially for low voltage generators which would cause the generator to often fail to operate correctly where it would oscillate at a single frequency due to the switch not consistently closing. This refers to a phenomenon where when the switch is closed the contacts bounce off of one another repeatedly until they settle into a closed position. Due to the single frequency waveform produced this was able to be handled by simply disregarding single frequency waveform results. This problem is not commonly faced and seems to not have been documented in other efforts as high-voltage testing rarely suffers from this due to arcing after initial contact – or the use of solid-state switching.

Over the course of the experimental research, switching characteristics and switch bounce were a common obstacle. While switch bounce can be minimized by testing at high voltage, use of triggered spark gaps or solid-state switches would eliminate this problem completely. Use of these switches will be considered for future research and will most likely lead to the use of triggered spark gaps to avoid limitations in the design of future spiral generators for testing. Winding of generators was also a major obstacle, without access to industrial grade winding systems it was required to design a winding system to ensure quality windings. This was mostly successful, but this system will need to be improved to allow a larger range of generators to be fabricated with more ease, accuracy,

and more uniform windings. The wish to simply and quickly design generators that would work well with most switches led to the development of the physics model referred to as the simple two-frequency model. This model alongside other methods and knowledge of generator design allowed easy design as it takes little effort to use and is accurate enough, but it does not help with fabrication methods.

The primary shortcoming of the simple model provided by the time dependent output waveform seen in Equation 3.14 is the inaccuracy of the resonant frequency f_r due to the dependence on the output capacitance. This can be followed back to the derivation of the output capacitance which would need to consider the generator multiplication efficacy ϵ_{ff} to be accurate. This shows that to produce a more accurate simple model for the behavior of the spiral generator accurate methodology to predict the multiplication efficiency must be developed. The output capacitance may not yet be the only factor in the inaccuracy of the resonant frequency, as switching effects are not accounted for in the equation for the resonant frequency. Great care should be taken when determining the output inductance as well, but trends suggest that most error results from an inaccurate output capacitance. As for the transit frequency, it is well accounted for in the case of the unloaded spiral generator. Load effects on wave propagation speed will need to be considered and may take the form of a ‘frequency damping’ factor determined by electrical characteristics of the load.

While the multiplication efficiency can be determined after fabrication and experimentation this is not ideal for designing spiral generators. It is desirable to be able to accurately calculate the multiplication efficiency and output behavior of the spiral generator prior to fabrication. This will hopefully allow more interest in the spiral generator

for economic purposes. A proposed path towards determining this efficiency would be to determine the efficiency factors first in terms of energy lost to resistance and inductance, before moving on to the others by eliminating some or all of the remaining efficiency factors.

Over the course of this exploration two generators were tested at both low and high voltage. These tests were primarily performed to further the authors' understanding of the workings of the spiral generators with the original intention of expansion to a parametric analysis. Difficulty in winding generators consistently without an industrial system designed for fabricating spiral generators led to a search for a less material alternative. This alternative came in the form of the simple model for the time-dependent behavior of the spiral generator.

5.4 Applications for Spiral Generators

Spiral generators can be used to produce a pulse that is not only high-voltage but has low jitter and consistent peak-to-peak timing. These generators can be designed and fabricated for specific timing and are programmable for different voltages. A common usage for these generators is for triggering or switching. The PT-55 spiral generator seen in *Figure 3.8* and *Figure 3.9* was used as the starting point for the DM-1 half power prototype now known as Charger One [35], [36]. It was used to trigger the system and considering the documentation's focus on precise timing the consistent peak-to-peak timing mentioned before is probably the reason it was used. Considering the modular design it is likely that each module of the Decade Quad contained one of these PT-55 components before it was decommissioned [37], [38].

While the Decade uses a spiral generator as a trigger, other X-ray sources have been developed using the spiral generator as the primary pulse producer and compressor and research by Ware *et al.* suggests these could be much more affordable due to lack of water or oil lines [12], [13], [39]. Some other applications involve rep-rated power and power for high-power microwave plasma sources which have been created by a few research efforts to operate as an RF oscillator or RF source for plasma sources [28], [30], [34], [40]. A less impressive but practical use is using spiral generators to start objects like HID lamps – which is useful due to their cheap cost and rugged solid-state designs [41]. Uses like this may point to other more wide-spread applications in infrastructure or consumer products.

5.5 Conclusions of Experimental Results

For results starting with those of the winding system, the system fabricated is simple and easy to construct. It can produce generators of decent consistency but should a different width or diameter be desired the entire system effectively has to be rebuilt from scratch. The first two generators in Table 4.1 are the two fabricated for this study that are referred to as the 30-turn and 52-turn spiral generator respectively. These generators only suffered minor issues during fabrication such as folding of the insulation. From the fabrications a suggested generator geometry is 25-35 turns on a 5-inch mandrel as that seemed to work well. A simple tension control system is discussed in Section 5.7 as part of a possible future winding system for future works. Addition of this or a similar system would allow much more flexibility in fabrication of spiral generators.

The experimentation on the generators went well. The low voltage experimentation of the 30-turn spiral generator produced consistent multiplication and waveforms being charged from 2V to 9V with multiplication efficiency ranging from 30.5% for the non-

switch bounce 4.1V case to 52% for the 9V case which produced 280V output voltage at peak. This is to be expected efficiency is to trend towards 50% for most geometries if switch characteristics are properly addressed.

5.6 Conclusions of Analytical Results

The simple time-dependent model offers a fairly accurate output waveform for the spiral generator. While exploring the different inductance methods it became apparent that the resonant frequency was the most influential source of error and that the transit frequency was within 5% of the expected value in most cases. The primary source of this error appears to be an incorrect calculation in the output capacitance. Using measured values rather than geometry to calculate the output capacitance results in a more accurate resonant frequency. This contrasts with using calculated values of output inductance using the method of choice in this study which usually results in less error than a measured value. This is true in most cases with outliers being cases of shorter coils such as those with lower mean diameters or number of turns. This is because the error is not only more emergent, but the electrical characteristic calculations become less accurate for small generators.

The simple two-frequency model was compared to the geometric analysis performed by Yan & Parker by utilizing their given geometric and measured electrical values [7]. These results are significant in that it shows that all required inputs for the model can be determined before the generator is built, and in many cases are more accurate than the analytical results of the much more complex model used by Yan & Parker and developed by Pal'chikov [7], [11]. It is important to note that Pal'chikov's model was meant to show multiplication efficiency while the simple two-frequency model only shows the shape of the output waveform relative to time-dependent behavior. Though it does show

some scaling of the output voltage independent of multiplication efficiency. In terms of qualitative comparison, the focus will be on timing of the first peak of each of the waveforms in the geometric analysis and will be compared to results using only calculated values from geometric parameters. For the scaling of turns, Yan and Parker produced experimental results resulting in a first turn time of approximately 60 ns, 90 ns, 120 ns, and 150 ns. Their analytical model discussed in Chapter 3 predicted these peaks at approximately 60 ns, 120 ns, 150 ns, and 160 ns respectively. The simple two frequency model predicts these peaks at 60 ns, 90 ns, 115 ns, and 130 ns respectively. In this respect the models despite their differences in complexity agree well with one another and the experimental results, however it should be noted that the results of Yan and Parker using Pal'chikovs model produce much wider waveforms and their amplitude scaling closely resembles ours. There is similar agreement to the cases for changing width or mean diameter but in most cases the simple two-frequency model produces waveforms that are more similar to the experimental waveform than those produced by Pal'chikov's model. There is one exception of the model for changing widths in which the two frequency model predicts all peaks at 90 ns whereas the experimental model and the results produced by Yan and Parker show the first peaks at 110-120ns. This gap may be due to an apparent 10-15 ns delay before their waveform begins to rise whereas the waveform the two-frequency model produced rises immediately. There appears to be a similar 10-15 ns delay on the results for changing mean winding diameter as well. Accounting for this would bring the comparison for all three results within 10% of one another.

5.7 Final Thoughts

While performing the research described in this work and reading for the literature survey, it became quickly apparent that there was no well-known or widely used means of determining the efficiency of the spiral generator that did not use experimental means. This was in addition to the lack of models with accurately describe the behavior of the spiral generator. The solution to the latter was the simple two frequency model. This model is already capable of producing a decent depiction of the output waveform of a spiral generator using only calculated values. This is with exception to loading effects on wave propagation speed and the multiplication efficiency of the generator. The simplicity of this model not only allows for an easy prediction of the shape of the output waveform but could also be modified with the intention of producing a derivation of the multiplication efficiency. The transit frequency could also be replaced with a function of time to account for the effects of wave propagation speed. This makes way for future work in terms of simple but cumulative operations to allow for a more accurate description of the behavior of the spiral generator by addressing the above two concerns. This will likely take the form of determining factors which alter wave propagation speed, determining an equation for the change in electrical characteristics such as inductance and input capacitance from corona, and development of equations or numerical methods for expressing the other four efficiency factors. For wave propagation it may take the form of the frequency damping factor described earlier, and function similarly to RLC damping factors for frequency rather than amplitude. For the efficiency factors a direction may be to replace one or more of the efficiency factors such as the third efficiency factor with time-based equations for the discharge of the energy stored in the charged conductor. Finally, problems with the

fabrication process led to a desire to develop a simple and easy to construct winding machine. That will also be possible future work, and a rough sketch of an addition to the design design can be seen in *Figure 3.13*.

References

- [1] J. Mankowski and M. Kristiansen, “A review of short pulse generator technology,” *IEEE Transactions on Plasma Science*, vol. 28, no. 1, pp. 102–108, 2000, doi: 10.1109/27.842875.
- [2] J. Jess and H. W. SchÜSslee, “On the Design of Pulse-Forming Networks,” *IEEE Transactions on Circuit Theory*, vol. 12, no. 3, pp. 393–400, 1965, doi: 10.1109/TCT.1965.1082451.
- [3] M. Shinagawa, Y. Akazawa, and T. Wakimoto, “Jitter analysis of high-speed sampling systems,” *IEEE J Solid-State Circuits*, vol. 25, no. 1, pp. 220–224, 1990.
- [4] R. A. Fitch and V. T. S. Howell, “Novel principle of transient high-voltage generation,” in *Proceedings of the Institution of Electrical Engineers*, 1964, vol. 111, no. 4, pp. 849–855.
- [5] A. Ramrus and F. Rose, “High-Voltage Spiral Generators,” Nov. 1976.
- [6] I. J. Cohen, E. Glynn, A. King, Z. Roberts, and M. Heffernan, “Evaluation of Liquid Dielectrics to Improve Spiral Generator Lifetimes,” Mar. 2022, pp. 1–7. doi: 10.1109/ppc40517.2021.9733136.
- [7] J. Yan, S. Parker, and S. Bland, “An Investigation into High-Voltage Spiral Generators Utilizing Thyristor Input Switches,” *IEEE Trans Power Electron*, vol. 36, no. 9, pp. 10005–10019, Sep. 2021, doi: 10.1109/TPEL.2021.3063499.
- [8] F. W. Grover, *Inductance calculations: working formulas and tables*. Courier Corporation, 2004.
- [9] F. Rühl and G. Herziger, “Analysis of the spiral generator,” *Review of Scientific Instruments*, vol. 51, no. 11, pp. 1541–1547, 1980, doi: 10.1063/1.1136120.
- [10] M. F. Rose, Z. Shotts, and Z. Roberts, “HIGH EFFICIENCY COMPACT HIGH VOLTAGE VECTOR INVERSION GENERATORS.”
- [11] E. I. Palchikov, A. M. Ryabchun, and T. Y. Bashkatov, “On the refinement of the theoretical model for a high-voltage spiral generator,” *Technical Physics*, vol. 52, no. 12, pp. 1597–1603, Dec. 2007, doi: 10.1134/S1063784207120122.
- [12] E. I. Pal’chikov, A. M. Ryabchun, and I. Y. Krasnikov, “Modified spiral high-voltage generator for feeding a pulsed X-ray apparatus,” *Technical Physics*, vol. 57, no. 2, pp. 292–301, Feb. 2012, doi: 10.1134/S1063784212020193.
- [13] E. I. Pal’chikov, A. v. Dolgikh, V. v. Klypin, A. M. Ryabchun, and M. S. Samoylenko, “Pulse X-ray Device Based on a Combined Spiral Generator,” *Journal of Applied Mechanics and Technical Physics*, vol. 60, no. 3, pp. 586–591, May 2019, doi: 10.1134/S0021894419030222.

- [14] J. Hanlon, Z. Shotts, M. F. Rose, and S. Best, “HIGH VOLTAGE SOLID STATE SWITCHED VECTOR INVERSION GENERATORS,” 2007.
- [15] J. Yan, S. Parker, T. Gheorghiu, N. Schwartz, S. Theocharous, and S. N. Bland, “Miniature solid-state switched spiral generator for the cost effective, programmable triggering of large scale pulsed power accelerators,” *Physical Review Accelerators and Beams*, vol. 24, no. 3, Mar. 2021, doi: 10.1103/PhysRevAccelBeams.24.030401.
- [16] R. A. Fitch, “Marx - and marx-like - high-voltage generators,” *IEEE Trans Nucl Sci*, vol. 18, no. 4, pp. 190–198, 1971, doi: 10.1109/TNS.1971.4326339.
- [17] K. R. LeChien and J. M. Gahl, “Investigation of a multichannelling, multigap Marx bank switch,” *Review of Scientific Instruments*, vol. 75, no. 1, pp. 174–178, Jan. 2004, doi: 10.1063/1.1630834.
- [18] N. G. Mutnitskii and V. v. Tatur, “A generator with a voltage inversion and output pulse amplitude doubling,” *Instruments and Experimental Techniques*, vol. 54, no. 6, pp. 778–780, Nov. 2011, doi: 10.1134/S0020441211050228.
- [19] T. G. Engel, K. Christian, and W. C. Nunnally, “High-Voltage Pulse Production Using Transformer-Coupled LC Vector Inversion Generators,” *IEEE Transactions on Plasma Science*, vol. 28, no. 5, pp. 1377–1381, 2000, doi: 10.1109/27.901201.
- [20] R. Bischoff, “An Alternative Circuitry for a Transformer-Coupled LC Inversion Generator,” *IEEE Transactions on Plasma Science*, vol. 48, no. 10, pp. 3424–3428, Oct. 2020, doi: 10.1109/TPS.2020.3016949.
- [21] J. Lehr and P. Ron, *Foundations of Pulsed Power Technology*. Piscataway, NJ: IEEE Press, 2017.
- [22] J. Liu, Y. Zhang, Z. Chen, and J. Feng, “A compact 100-PPS high-voltage trigger pulse generator,” *IEEE Trans Electron Devices*, vol. 57, no. 7, pp. 1680–1686, Jul. 2010, doi: 10.1109/TED.2010.2047905.
- [23] D. Bhasavanich, S. S. Hitchcock, P. M. Creely, R. S. Shaw, H. G. Hammon, and J. T. Naff, “Development Of A Compact, High-energy Spark Gap Switch And Trigger Generator System,” Aug. 2005, pp. 343–345. doi: 10.1109/ppc.1991.733302.
- [24] Z. Shotts, Z. Roberts, and M. F. Rose, “Limits and failure modes in High Voltage Vector Inversion Generators.”
- [25] Z. Shotts, Z. Roberts, and M. F. Rose, “Design Principles for Vector Inversion Generators,” 2007.
- [26] S. I. Shkuratov *et al.*, “Completely explosive autonomous high-voltage pulsed-power system based on shockwave ferromagnetic primary power source and spiral

- vector inversion generator,” in *IEEE Transactions on Plasma Science*, Oct. 2006, vol. 34, no. 5 I, pp. 1866–1872. doi: 10.1109/TPS.2006.883347.
- [27] S. I. Shkuratov *et al.*, “Completely explosive ultracompact high-voltage nanosecond pulse-generating system,” *Review of Scientific Instruments*, vol. 77, no. 4, 2006, doi: 10.1063/1.2168674.
- [28] Z. Roberts, Z. Shotts, and M. F. Rose, “Ultra-Compact high efficiency multi-kilovolt pulsed power source.”
- [29] Y. Zhang *et al.*, “A compact high-voltage pulse generator based on pulse transformer with closed magnetic core,” *Review of Scientific Instruments*, vol. 81, no. 3, 2010, doi: 10.1063/1.3321494.
- [30] Z. Roberts, Z. Shotts, and M. F. Rose, “PPPS-2007: DESIGN AND TESTING OF A VECTOR INVERSION GENERATOR OPERATING AS A RF OSCILLATOR,” 2007.
- [31] S. A. Merryman, M. Frank Rose, and Z. Shotts, “Characterization and applications of vector inversion generators,” in *Digest of Technical Papers-IEEE International Pulsed Power Conference*, 2003, pp. 249–252. doi: 10.1109/ppc.2003.1277703.
- [32] Z. Shotts, “Personal Communication.” Jul. 30, 2022.
- [33] N. v Belkin and A. Y. Zharkova, “USSR Inventor’s Certificate No. 149 494,” *Byull. Izobret*, no. 16, p. 35, 1962.
- [34] Z. Shotts and M. F. Rose, “High voltage solid state switched vector inversion generator for HPM applications,” in *PPC2009 - 17th IEEE International Pulsed Power Conference*, 2009, pp. 908–912. doi: 10.1109/PPC.2009.5386220.
- [35] “(5) Overview of Charger1_JasonCassibry”.
- [36] P. Sincerny *et al.*, “Performance of decade module #1 (DM1) and the status of the decade machine,” in *Digest of Technical Papers-IEEE International Pulsed Power Conference*, 1995, vol. 1, pp. 405–416. doi: 10.1109/ppc.1995.596513.
- [37] P. Sincerny, S. Ashby, K. Childers, C. Deeney, and L. Schlitt, “THE DECADE HIGH POWER GENERATOR,” Aug. 2005, p. 880. doi: 10.1109/ppc.1993.514063.
- [38] “(8) DECADE QUAD DESIGN AND TESTING STATUS_P_SINCERNY”.
- [39] K. Ware, R. Gullickson, J. Pierre, R. Schneider, and I. Vitkovitsky, “TECHNOLOGIES FOR DEVELOPMENT OF MORE AFFORDABLE LARGE X-RAY SIMULATORS.”
- [40] Y. Wu, J. P. Hurley, Q. Ji, J. W. Kwan, and K. N. Leung, “Sealed operation of a rf driven ion source for a compact neutron generator to be used for associated particle

imaging,” in *Review of Scientific Instruments*, 2010, vol. 81, no. 2. doi: 10.1063/1.3266114.

- [41] J. N. Lester, J. M. Proud, and C. N. Fallier, “Starting HID Lamps with Spiral Line Pulse Generators,” *Journal of the Illuminating Engineering Society*, vol. 16, no. 1, pp. 72–80, 1987.